

POLITECNICO DI TORINO

MSc's Degree in MECHATRONIC ENGINEERING



MSc Degree Thesis

**Design and Development of a Retrofitting
system for waste collection vehicles
enabling predictive maintenance
applications**

Supervisors

Prof. Marco VACCA

Candidate

Daniel Pablo TRIGO NAGEL

July 2022

Summary

The following project is focused on the design and implementation of a predictive maintenance system for a hydraulic system of a waste collection truck. This thesis is an outcome of the collaboration with the Competence Industry Manufacturing 4.0 of Torino, which at the same time collaborated for this project with the company SEA Ambiente, which is in charge of collecting the waste of different city locations.

After taking the Failure Mode and Effects Analysis of the hydraulic system provided by the SEA company. Two main failures were identified, the first one is oil leakage in the hydraulic cylinders and the second wear in the rail pads where the hydraulic actuators perform a linear displacement for trash compaction.

Using the detected failures as a starting point for the predictive maintenance procedure. A set of sensors was selected in order to help with the detection, analysis of failures in the system and further causalities which lead to oil leakage in the system cylinders. The selected sensors are the following:

- An oil health monitoring sensor for contaminant particle detection.
- A pair of ultrasonic distance measure sensors for detecting the level of oil in the reservoir for big leakage amounts.
- A pair of pressure sensors for small leakage detection.
- A temperature sensor for detecting internal fluid overheating in the system.
- A pair of accelerometers for failure detection of the rail pads where the hydraulic actuators perform a linear displacement.
- A couple of inductive sensors to detect the wear in the Teflon rail pads which help with the sliding operation of the hydraulic actuators in the rails.

For the Data acquisition system an Arduino Mega 2560 and a Raspberry Pi 4 boards were used, the Arduino board processed the data of all the sensors except the accelerometers which were processed by the Raspberry Pi due to the high data rate, SERIAL communication was used with the boards and the sensors. The data acquisition system contained the following modules:

- Battery module, which provides the power for the data acquisition system.
- Binary signals module which correspond to the signals already implemented on the truck for the hydraulic system operation
- Sensors Module which contains all the previous mentioned sensors.
- 4G Router module which sends the collected sensor data via WiFi connection to a cloud
- The SEA BOX module where was implemented the Arduino and Raspberry connection with the sensors . Also it was implemented a power distribution module to distribute the power to all the system components and a signal conditioning module to process the binary signals of the hydraulic system.
- A GNSS module which was also installed in order to send the car location in real time.

Since the real system needed time to obtain failure data, a model based approach of the hydraulic system was also developed using Simscape, which operates in the Simulink environment, such dynamic model simulated normal operating conditions and failure conditions of the hydraulic system where internal and external leakages are modelled and simulated for data acquisition and later analysis.

The pressure signal was used to detect small internal and external leakage of the hydraulic cylinder with signal processing techniques, two techniques were used, Wavelet transform and Hilbert Huang transform the leakage detection was done comparing RMS values of healthy and faulty conditions of the system

Acknowledgements

I would like to thank God first of all for giving me the possibility and opportunity of having the beautiful experience of this master degree. I would like to dedicate my work to my wife, daughter and my family in Bolivia (parents and brothers), without their constant support this thesis would not have been possible, I owe them in full gratitude and love.

My gratitude goes to the Competence Industry Manufacturing 4.0 of Torino and Eng. Orlando Tovar and Eng. José Guarino, both helped me and supported my work during all this period with their knowledge and experience. Finally thank also professor VACCA who accepted being my thesis relator.

Table of Contents

List of Tables	IX
List of Figures	X
1 Introduction	1
1.1 Description of the hydraulic compactor system	1
1.1.1 System Components	2
1.2 Description of the problem	7
1.2.1 Failures related to the handling of the compaction bulkhead	7
1.2.2 Failures related to wear of the Teflon sliders	8
1.3 Objectives of the Thesis	8
1.4 Project Scope	9
2 Failure Mode and Effect Analysis	10
2.1 Elements of FMEA	11
2.1.1 Basic definitions	11
2.1.2 Risk Priority Number RPN and Criticality values	12
2.2 FMEA Methodology	15
2.3 FMEA of SEA company	15
3 Failure detection procedures and techniques	18
3.1 Machine maintenance	18
3.2 Hydraulic systems fault types	19
3.2.1 Oil leakage in hydraulic systems	19
3.2.2 Oil leakage monitoring methods in hydraulic systems	20
3.2.3 Particle contamination in hydraulic systems	22
3.2.4 Particle contamination monitoring methods in hydraulic systems	23
3.3 Teflon rail pads wear fault	24
3.3.1 Monitoring rail pads Teflon sliders	24
3.3.2 Misalignment of the cylinders	24

3.4	Description of sensors	25
3.4.1	Pressure sensors	25
3.4.2	Temperature sensors	25
3.4.3	Oil level monitoring sensor	28
3.4.4	Oil health monitoring sensor	29
3.4.5	Accelerometer for cylinder misalignment	31
3.4.6	Teflon sliders wear sensors	32
4	Data acquisition system	34
4.1	High level description of the system	35
4.2	SEA Box description	37
4.2.1	Signal conditioning module	37
4.2.2	Power supply and power distribution system	39
4.2.3	Analog Sensor modules	40
4.2.4	Accelerometer box STWINKT1B	46
4.2.5	4G GNSS module	47
4.2.6	Data processing	47
4.2.7	Log protocol	48
4.2.8	Saving Data	53
5	Methodological implementation for leakage detection	54
5.1	Hilbert Huang transform methodology	54
5.1.1	Empirical Mode Decomposition	54
5.1.2	Hilbert-Huang spectrum	57
5.2	Wavelet transform methodology	58
5.3	Predictive Maintenance Algorithm development	59
5.3.1	Data Acquisition	59
5.3.2	Data pre-processing	60
5.3.3	Condition Indicators	60
6	System modelling for data acquisition	61
6.1	Hydraulic cylinder leakage Modelling	62
6.1.1	Control Valve analysis	62
6.1.2	Hydraulic cylinder dynamic modelling	66
6.2	Matlab System Modelling	69
7	System simulation, fluid leakage detection and final results	73
7.1	External leakage	73
7.2	External Leakage simulation	74
7.2.1	External leakage results	76
7.3	Internal leakage	79
7.3.1	Internal leakage Wavelet decomposition results	82

7.3.2 Internal leakage Hilbert-Huang decomposition results	86
8 Conclusions and further works	91
A Matlab Code external leakage detection	93
B Matlab Code Internal leakage detection	99
Bibliography	107

List of Tables

2.1	Severity guidance for systems FMEA	13
2.2	Occurrence guidance for systems FMEA	14
2.3	Detection guidance for systems FMEA	14
2.4	First section of SEA FMEA	16
2.5	Second section of SEA FMEA	17
2.6	Third section of SEA FMEA	17
7.1	First experiment results with WT methodology for external leakage detection	77
7.2	First experiment results with WT methodology for internal leakage detection	86
7.3	First experiment results with HHT methodology for internal leakage detection	88

List of Figures

1.1	SEA hydraulic system operation	3
1.2	SEA hydraulic system schematic	4
1.3	Solenoid Control Valve	5
1.4	Pressure relief valve	6
1.5	view of the rail and Teflon wear section	8
2.1	Flowchart of FMEA methodology	16
3.1	Hydraulic system schematic with sensors	26
3.2	PT5501 IFM pressure sensor	27
3.3	Locations of installation of pressure sensor in the system	27
3.4	TA310 IFM temperature monitor	28
3.5	mic+25/IU/TC Microsonic Ultrasonic distance measure sensor	28
3.6	Oil level sensors location	29
3.7	LDP100 IFM optical particle monitor	30
3.8	C optical sensor installation	30
3.9	ST, STEVAL-STWINKT1B board	31
3.10	STEVAL-STWINKT1B board location in the system	32
3.11	Contrinex DW-Ax-509-M18-320 inductive sensor	32
3.12	Inductive sensor position	33
4.1	Arduino Mega 2560 board	35
4.2	Raspberry Pi 4	36
4.3	General schematic data acquisition system	36
4.4	Truck binary signals representation	39
4.5	Power supply module	40
4.6	Sequential data output via the analogue output	41
4.7	LDP100 sensor pinouts	42
4.8	LDP100 circuit schematic	42
4.9	PT5501 and TA3105 circuit	43
4.10	pressure sensor pinout	44

4.11	Temperature sensors pinout	44
4.12	mic+25/IU/TC circuit schematic	45
4.13	mic+25/IU/TC sensor pinouts	45
4.14	DW-AS-509-M18-320 circuit schematic	46
4.15	inductive sensor pinout	46
4.16	Accelerometer installation	47
4.17	Final data acquisition system	48
4.18	KuWFi CPF905 router	49
4.19	Accelerometers collected data	52
5.1	Algorithm development process	59
6.1	Four-way spool valve	63
6.2	Failure cylinder-valve system	67
6.3	Hydraulic system general modelling	71
6.4	Overview of subsystems	71
6.5	Valve-cylinder modelling	72
7.1	Pressure output with internal leakage	74
7.2	Wavelet decomposition, hydraulic cylinder with no leakage	76
7.3	Approximate coefficients of wavelet decomposition, hydraulic cylinder with small external leakage	77
7.4	Leakage measurement of the valve opened at 5 micrometers	78
7.5	Approximate coefficients of wavelet decomposition, hydraulic cylinder with medium external leakage.	79
7.6	Leakage measurement of the valve opened at 25 micrometers	80
7.7	External leakage detection results	81
7.8	healthy and fault conditions step response	82
7.9	Wavelet decomposition, approximation and detail coefficients, no leakage	83
7.10	Wavelet decomposition, approximation and detail coefficients, small leakage	84
7.11	Wavelet decomposition, approximation and detail coefficients, medium leakage	84
7.12	Wavelet decomposition, approximation and detail coefficients, large leakage	85
7.13	Internal leakage computation across the cylinder	85
7.14	WT internal leakage results	86
7.15	Empirical Mode Decomposition of the Pressure signal with no leakage	87
7.16	Instantaneous Amplitude of the estimated IMF's	88
7.17	IMF's of the Pressure signal with small leakage	89
7.18	IMF's of the Pressure signal with medium leakage	89

7.19 IMF's of the Pressure signal with large leakage	90
7.20 HHT internal leakage results	90

Chapter 1

Introduction

Different types of industries and service companies rely on a wide range of machines, such machines eventually present failures due to continuous usage. As a result, it is important to understand what are those failure effects on the operating process, moreover understand as well the causes of such failures in order to implement a proper detection system. Such measurements will allow the owner to firstly increase the operating life of the machine and in second place if the technology allows, to implement algorithms able to detect a failure when it begins, but the system is still operable, and repair it in a manageable time before it evolves to the point where it leads to a higher risk failure. Such idea will allow the owner to plan the machine maintenance while it is still in operating conditions.

The following thesis document grows in collaboration with CIM 4.0 Torino. The Competence Industry of Piedmont is works with different partner companies to bring to some industry sectors adequate technological solutions for different needs and purposes.

This project was executed as a partnership of CIM 4.0 with SEA Ambiente. SEA Ambiente is a company in charge of collecting waste in the city of Turin. Due to the high use of their truck fleet, many of the waste trucks present different types of failures, this document is focused in analyzing the hydraulic trash compaction system failures. It is important to focus on what are the effects of such failures in the system, what are the failure causes, and finally how can we detect them by means of sensor measurements, system modelling and signal processing techniques.

1.1 Description of the hydraulic compactor system

SEA has different types of vehicles for different functionalities, the vehicle which this project is focused on, is the FARID MICRO waste collection truck. Such

vehicle has the capability of operating in urban areas in a versatile way given its low dimensions, which makes it adequately to collect trash in low manoeuvrable areas of the city.

The hydraulic system of the truck performs a compaction operation of the collected waste, see Figure 1.1. As it is possible to see in the hydraulic schematic of the system in Figure 1.2, there are two main operations that the system performs. The first one, related to the shovel actuated by two short hydraulic cylinders which performs a circular movement from a point of rotation, such operation is in charge of raking the waste from the back section of the truck. The large compaction pistons are in charge of performing a linear displacement back and forward of the shovel from the front of the truck to its back and vice versa. The system functioning has the following stages:

- At the beginning the large cylinders are fully retracted, thus the shovel is at the front of the truck. The short cylinders are fully retracted, thus the shovel starts in horizontal position pointing towards the back of the truck.
- A command is given by the driver which is operating the system from the cabin. Once this is done, the short cylinders don't change the state. The large cylinders start their displacement taking the shovel to the back position of the truck.
- Once the shovel reaches the back position, a command is given to the short cylinders to fully extend rotating the shovel to a horizontal position, therefore the shovel is in vertical position pointing towards the ground. After this, the large cylinders start retracting. Thus, the waste is compacted by the shovel.
- When the large cylinders are again fully retracted, the short cylinders change the state from fully extended to fully retracted, thus the shovel changes from vertical position to horizontal. At this point the initial position is reached and the process can start again.

1.1.1 System Components

The system is composed by the following components.

- One Pump OMFB 10502300359
- Two control solenoid-valves with serial code L5211B201000000.
- One pressure relief valve HYDROVER H14006.
- A pair of hydraulic cylinders of 102 cm length.

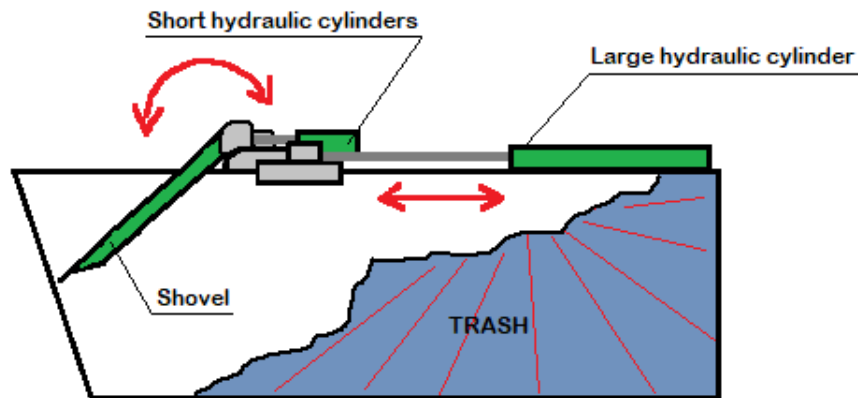


Figure 1.1: SEA hydraulic system operation

- A pair of hydraulic cylinders of 38 cm length.
- Hydraulic hoses Dunlop Hiflex.

In the following lines, the main characteristics of each component are presented.

Pump

The pump is in charge of generating high pressure on the system for the its functioning.

- Pump type: Gear pump, OMFB 10502300359
- Max. Continuous pressure: 280 bar
- Max. Peak Pressure: 310 bar
- Displacement: 33.88 cubic centimeters per revolution
- Max. continuous speed: 2200 rpm.
- Min. speed: 300 rpm.

Solenoid control valves

The solenoid DC control valves are two in total. The first one is in charge of controlling the short hydraulic cylinders, in charge of the rotation of the shovel. The second valve is in control of the large hydraulic cylinders that perform the linear displacement of the shovel.

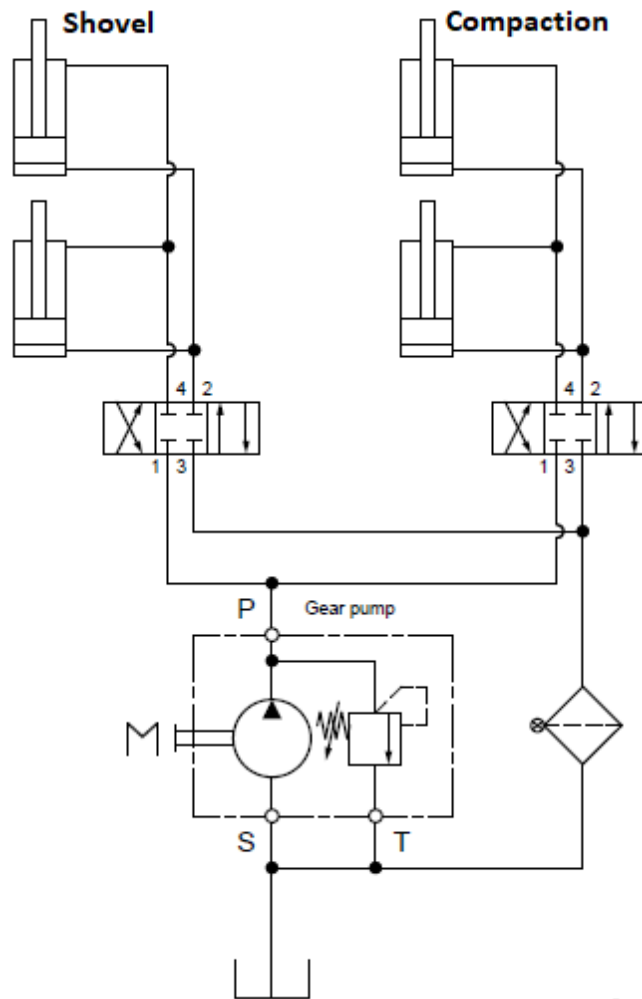


Figure 1.2: SEA hydraulic system schematic

- Valve type: 4 way 3 position solenoid valve, Oleodinamica LC, L5211B201000000
- Max. Flow: 120 L/min
- Max. Operating pressure on A-B-P: 310 bar
- Max. Operating pressure on T dynamic: 250 bar, see Figure 1.3
- Max. Operating pressure on T static: 300 bar, see Figure 1.3

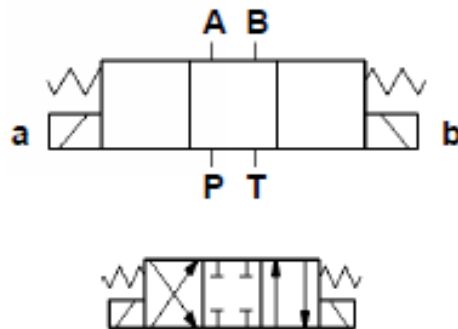


Figure 1.3: Solenoid Control Valve

Pressure relief valve

The pressure relief valve is in charge of protecting the system components from over pressure, releasing the system pressure when it reaches a maximum point, see Figure 1.4 . The valve used in the system is regulated to operate at a maximum pressure of 200 bar.

- Valve type: HYDROVER H14006
- Max. Pressure: 350 bar.
- Relief valve adjustment V1 and V2, see Figure 1.4 .
 - 25 - 120 bar
 - 40 - 200 bar
 - 200 - 350 bar

Large hydraulic cylinders

As previously mentioned, the large hydraulic cylinders are in charge of the waste compaction by linear displacement of the shovel.

Special emphasis must be taken to the fact that short and large hydraulic cylinders of the system are handmade, in contrast to the other elements of the system they are not subjected to exhaustive quality tests as the other components are. As a result, it will be seen later in the FMEA analysis which points directly to cylinder failures, rather than in the rest of the hydraulic components of the system.

- length of the cylinder: 102 cm.

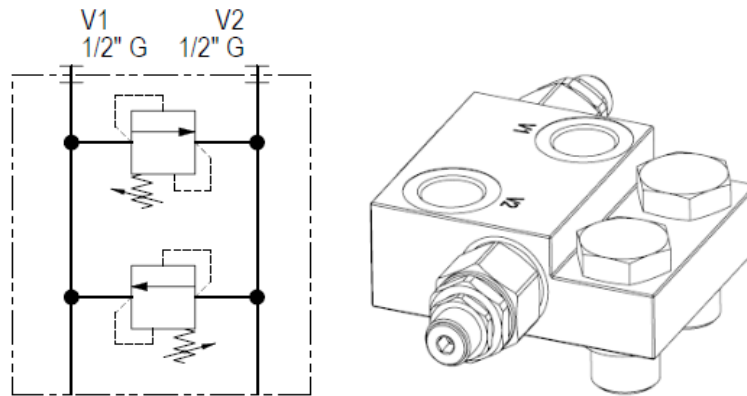


Figure 1.4: Pressure relief valve

- Outside diameter: 7 cm.
- Inner diameter: 6.5 cm.
- Rod diameter: 3 cm.
- Inlet oil diameter: 1 cm.
- Max. rod extension: 90 cm.
- Max. rod pressure: 300 bar.

Short hydraulic cylinders

This pair of cylinders are in charge of the rotation of the shovel. They rotate the shovel from a horizontal position to a vertical position, the vertical position has to be maintained while the compaction process, such process is performed by the linear displacement of large cylinders.

As mentioned previously also the short hydraulic cylinders are handmade.

- length of the cylinder: 38 cm.
- Outside diameter: 7 cm.
- Inner diameter: 6.5 cm.
- Rod diameter: 3 cm.
- Inlet oil diameter: 1 cm.
- Max. rod extension: 25 cm.
- Max. rod pressure: 300 bar.

Hydraulic hoses

The hoses allow the connection between the different hydraulic system components, letting the pressurized fluid circulate within the system for an appropriate functioning.

- Manufacturer: Hiflex.
- Max. Pressure: 345 bar.
- Inner diameter: 2 cm.

1.2 Description of the problem

As mentioned before, SEA uses a fleet of Farid micro vehicles. Due to usage, after a certain time of operating on a daily basis, each vehicle starts to present several types of failures. The faults related to the hydraulic compaction system are of particular interest and present the following common problems according to SEA technical operators:

- Failures related to the handling of the compaction bulkhead.
- Failures related to wear of the Teflon sliders or rail pads.

In the following two sections, the documentation of failures given by SEA is presented and analyzed in more detail.

1.2.1 Failures related to the handling of the compaction bulkhead

The system presents a high oil leakage rate in the shovel system and the bulkhead compaction system. The detection of leakage most of the times is noticed by the movement of the two pistons, an appreciable loss of pressure can only be detected when there is no longer sufficient oil for the complete movement of the pistons and the damage is already evident due to the impossibility of operating. It is possible, but not taken for granted, that there is also a possible correlation with the temperature of the oil itself.

The loss of oil used for the distribution of force to the equipment is typically due to the system wear, according to the FMEA presented in Chapter 2 the leakages are mostly presented in the cylinders, however the SEA personnel also mentioned the oil leakage in a lesser degree is also due to breakage of pipes, sleeves, fittings and loss of seal of any gaskets, however in this project such leakages will not be considered.

1.2.2 Failures related to wear of the Teflon sliders

The hydraulic system which pushes the compaction bulkhead slides on steel rails, the hooks that move horizontally on the rails, have a Teflon coating to facilitate their sliding. The problem of the compaction bulkhead system arises from the wear of the Teflon of the upper section of the hook to the rail. This material allows the hitch to slide easily thanks to the thrust of the hydraulic piston. The wearing section of Teflon is coloured in yellow in Figure 1.5.

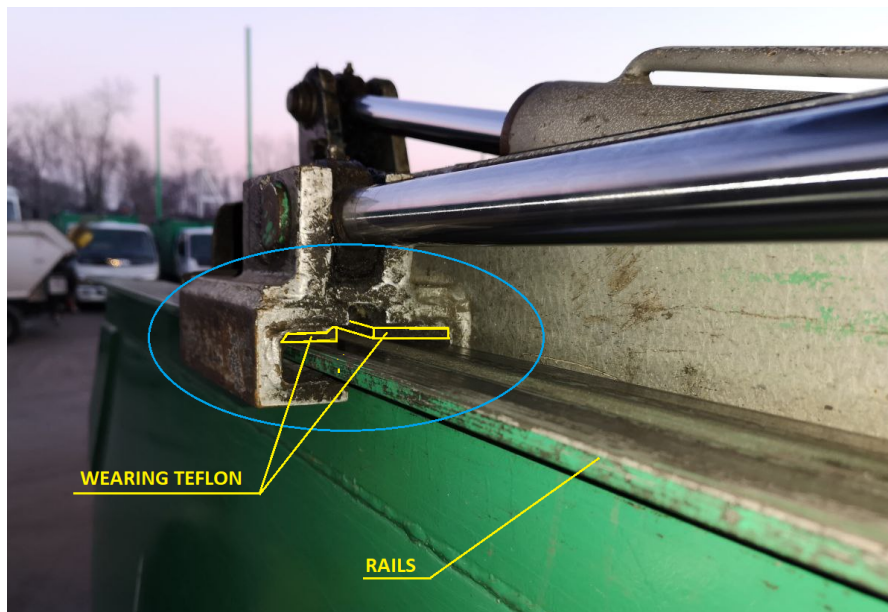


Figure 1.5: view of the rail and Teflon wear section

1.3 Objectives of the Thesis

The main objective of this project is the following:

- The analysis of the most common failure causes.
- The design of a system capable of detecting failures (rails and leakage) in advance, preventing them from evolving into more critical faults that could damage other components, leaving the system inoperable.

1.4 Project Scope

The following thesis project presents a review, design and implementation of predictive maintenance state of the art developments for hydraulic systems. A selection of different types of sensors based on the project constraints and bibliographic material.

Chapter 2 describes the foundations of FMEA analysis, describing key definitions and FMEA methodology which explains how to proceed in order to do a correct FMEA analysis. It ends up presenting an already elaborated FMEA analysis by SEA for the current project.

Once the FMEA is presented, Chapter 3 introduces in a first section, the most common causes for leakage failures in hydraulic systems only putting emphasis in hydraulic cylinders. Since as previously mentioned the hydraulic cylinders used in the trucks are handmade, in contrast with the rest of the system components. Chapter 3 also introduces the state of the art methods that can be used in order to detect leakages in hydraulic cylinders. Chapter 3 doesn't with a methodology able to detect leakages in pumps, servo-valves and other components of the system, the methodology presented could be useful for such purposes, however only hydraulic cylinders were taken into account in the analysis. In the second part it introduces the sensors that will be used for this project in order to detect leakages in the system, the wear of Teflon rail pads and also to monitor the health quality of the oil.

Chapter 4 describes the data acquisition system design, done in collaboration with an engineer provided by C.I.M. 4.0 for this project from the hardware perspective only, the scripts of the data acquisition system boards are not described in this project since they were performed by the engineer assistant and were not contemplated to be part of this thesis work.

Since leakage is the only fault problem that not only requires sensors to take measurements but also a signal processing and an algorithmic approach to detect small amounts of oil leakage, Chapter 5 introduces a methodological implementation for leakage detection using Hilbert Huang transform and Wavelet transform, both are signal processing techniques capable to detect variations in the system dynamics.

The data acquisition system has not yet been able to take measurements of the system operating in faulty conditions, for such reason chapter 6 introduces a mathematical modelling approach that was used to model and simulate the dynamic behavior of hydraulic system operating with leakage faulty conditions in order to take measurements and apply the signal processing techniques described in chapter 5.

Finally Chapter 7 uses the simulated data and presents the results of detection of internal and external oil leakages in the cylinders of the system using the already proposed methodologies.

Chapter 2

Failure Mode and Effect Analysis

Failure Mode and Effects Analysis FMEA is a common engineering procedure used in a number of industries in order to conduct analysis of the system, subsystems or processes, potential failures, problems or errors. FMEA is used to assess the risk associated with those failure modes, to rank the issues in terms of importance and to identify corrective actions to address the most serious concerns and prevent failures, as a result the idea is to improve as much as possible the durability, reliability and quality.

The FMEA analysis in this thesis project was used as a starting point to determine the most common failures modes in the truck compaction hydraulic system and evaluate each of them according to their criticality. In such format, different actions were taken to tackle the common machinery faults with possible solutions.

According to [1], the FMEA is characterized by the following aspects:

- Identifies known and potential failure modes.
- Identifies the causes and effects of each failure mode.
- Prioritizes the identified failure modes according to the risk priority number (RPN), which it will be detailed later, but essentially it is the product of frequency of occurrence, severity, and detection.
- Provides for problem follow-up and corrective action

2.1 Elements of FMEA

It is important to understand some key concepts in order to elaborate properly any system, design, process, component, subsystem, service FMEA.

2.1.1 Basic definitions

Function. Since the FMEA is focused in detecting failure modes of not only an entire system, but also subsystems, processes, components, etc. It is of paramount importance to have a clear idea of the task performed by each one of them. This has to be communicated in a clear manner. Such work is very important to understand the entire FMEA process.

Failure. In general, people have an idea of what a failure could be. In this case it is not far from the general understanding. A failure is the problem, error, concern, etc. that a system, subsystem, process, component, etc. presents. This notion comes from the expectations of the customer or even the designer of the machine. For instance if the machine is not working according to specifications or design purposes, this may be because there could be an inherent error (failure) in the system.

Failure Mode.

This is the physical description of the manner in which a failure occurs. In other words it is the manner in which a system, subsystem, or component fails to meet the intended purpose or function. Examples of failure modes are some of the following: Open circuit, leak, hot surface, etc.

It is very important to understand that a failure mode may have more than one level depending on the complexity of the defined function, this means that more levels of analysis can be performed for different types of failure modes.

Effects of failure. It deal with the description of the impact of a Failure Mode on the system, subsystem, process, or component. In more simple words, the Effects of Failure answer the question of what will happen if such failure occurs, it deals with the consequences of such failure from a description point of view. Answering such questions may require a deep knowledge of the system, subsystem, component, etc. under analysis.

One must understand, however, that the effects of the failure must be addressed from two points of view. The first viewpoint is local, in which the failure is isolated and does not affect anything else. The second viewpoint is global, in which the failure can and does affect other functions or components. In many cases it has a domino effect. Generally speaking, the failure with a global effect is more serious than the one of local nature.

The effect of the failure also will define the severity of a particular failure. In fact, the effect of the failure has a direct relationship with severity. So if the effect

is serious, the severity will be high. Examples of effects of failure follow.

- Local: light bulb failure
- Global: Power steering failure

Causes of Failure. This can be referred as the "how" of "why" of a failure, in other words what is the root cause of the listed failure. It is generally provided as a description of the factors contributing to the Failure Mode. Cause of failure is perhaps the most important section of the FMEA. This is where it is needed to point the way towards preventive and/or corrective action. The more focused on is on the root cause, the more successful will be the elimination failures. When dealing with preventive and/or corrective action it is important not to provide a very fast, quick or even easy solution. In some cases a quick solution may result in becoming a victim of symptoms and short-term remedies, rather than a complete elimination of the real problems.

Detection Method. (Failure Control) Refers to those methods and controls associated with standard practice and includes customary methods, practices, techniques and tests used by the producer (or system designer) to detect or control the failure cause.

2.1.2 Risk Priority Number RPN and Criticality values

The essence of the FMEA is to identify and prevent known and potential problems. To do that some assumptions have to be made, one of which is that problems have different priorities. For such reason the Failure Effect, The failure cause and the Failure Detection are ranked. There are three components that help define the priority of failures:

- Severity (S).
- Occurrence (O).
- Detection (D).

For such purpose the person that is performing the FMEA analysis, looks at what is the severity of the effect, what is the occurrence of the cause and looks at the ability to detect such failure.

A ranking for the criteria can have any value. The ranking of 1 to 10 is used widely and, in fact, is highly recommended because it provides ease of interpretation, accuracy, and precision in the quantification of the ranking. In this work it was adopted the 1 to 10 scale for more contrast between different failures.

Severity is the rating of the seriousness of the effect of a failure mode to system, subsystem, component, etc. See Table 2.1 Severity guidance for systems FMEA.

Effect	Rank	Criteria
None	1	No Effect
Slight	2	Customer not annoyed. Very slight effect on product or system performance
Very Slight	3	Customer slightly annoyed. Slight effect on product or system performance
Minor	4	Customer experiences minor nuisance. Minor effect on product or systems performance
Moderate	5	Customer experiences some dissatisfaction. Moderate effect on product or system performance
Significant	6	Customer experiences discomfort. Product performance degraded, but operable and safe. Partial failure, but operable.
Major	7	Customer dissatisfied. Product performance severely affected but functional and safe. System impaired.
Extreme	8	Customer very dissatisfied. Product inoperable but safe. System inoperable.
Serious	9	Potential hazardous effect. Able to stop product without mishap - time dependent failures. Compliance with government regulation is in jeopardy.
Hazardous	10	Hazardous effect. Safety - related - sudden failure. Noncompliance with government regulation.

Table 2.1: Severity guidance for systems FMEA

Occurrence is the rating of the cumulative number of failures that could occur over the design life of a system, subsystem, component, etc. normally per thousand operating times of usage or per hours. See Table 2.2 Severity guidance for systems FMEA.

Detection is the rating of the ability of the proposed design control to detect a potential failure mode or occurrence, before it puts the system operation in jeopardy. See Table 2.3 Detection guidance for systems FMEA.

Risk Priority Number

The priority of the problems presented is articulated via the RPN. This number is a product of the occurrence, severity, and detection. The value by itself should be used only to rank order and concerns of the system, design, product, process, and service.

$$RPN = Occurrence * Severity * Detection = O * S * D \quad (2.1)$$

After the RPN has been determined, the evaluation begins based on the definition

Effect	Rank	Criteria	CNF/1000
Almost Never	1	Failure unlikely, history shows no failures	<.000058
Remote	2	Rare number of failures likely	.0068
Very Slight	3	Very few failures likely	.0063
Slight	4	Few failures likely	.46
Low	5	Occasional number of failures likely	2.7
Medium	6	Medium number of failures likely	12.4
Moderately High	7	Moderately high number of failures likely	46
High	8	High number of failures likely	134
Very High	9	Very High number of failures likely	316
Almost Certain	10	Failure almost certain. History of failures exists from previous or similar designs	>316

Table 2.2: Occurrence guidance for systems FMEA

Effect	Rank	Criteria
Almost certain	1	Proven detection methods available while in conceptual design
Very High	2	Has very high effectiveness
High	3	Has high effectiveness
Moderately High	4	Has moderately high effectiveness
Medium	5	Has medium effectiveness
Low	6	Has low effectiveness
Slight	7	Has very low effectiveness
Very Slight	8	Has lowest effectiveness in each applicable category
Remote	9	Unproven, or unreliable, or effectiveness is unknown
Almost impossible	10	No technique is available or known, and/or none is planned

Table 2.3: Detection guidance for systems FMEA

of the risk. Usually this risk is defined by the team as minor, moderate, high, and critical. It may be changed to reflect different situations.

- Under minor risk, no action is taken.

- Under moderate risk, some action may take place
- Under high risk, definite action will take place. (Selective validation and evaluation may required).
- Under critical risk, definite actions will take place and extensive changes are required in the system, design, product, process, and/or service.

If there are more than two failures with the same RPN, then first address the failure with high severity, and then detection. Severity is approached first because it deals with the effects of the failure. Detection is used over the occurrence because it is customer dependent.

Criticality of failure Criticality is is the relative measure of the combined influences for the system failure. Based upon some severity level and some number of times it occurs, what it tells is how overall this failure mode is to the operation of our system. So what it is done is to take that number, that severity number, we take the occurrence number. The criticality value is given by the following expression.

$$Criticality = O * S \tag{2.2}$$

The long term goal is to completely eliminate every single failure. The short term goal is to minimize the failures if not eliminate them. Of course, the perseverance for those goals has to be taken into consideration in relationship to the needs of the organization, costs, customers, and competition.

2.2 FMEA Methodology

In the methodology for developing and FMEA, the team in charge of such process has to rank the failure effect, the failure cause and the failure detection method. As a result attention has to be pointed towards Severity, which ranks the failure effect, Occurrence which ranks the failure cause, and Detectability which ranks the detection method. Figure 2.1 describes such process.

2.3 FMEA of SEA company

SEA has developed its own FMEA, which is divided in different tables. Table 2.4 has the Name of the components that were analyzed, the Function where the specific functionality of a component is described, the Failure Modes are specified and the Failure effects are developed. Finally the ranking of failure effects by means of Severity. Table 2.5, describes the Failure Causes ranked by the Occurrence factor, the failure detection ranked as well by the Detection factor and Table 2.6

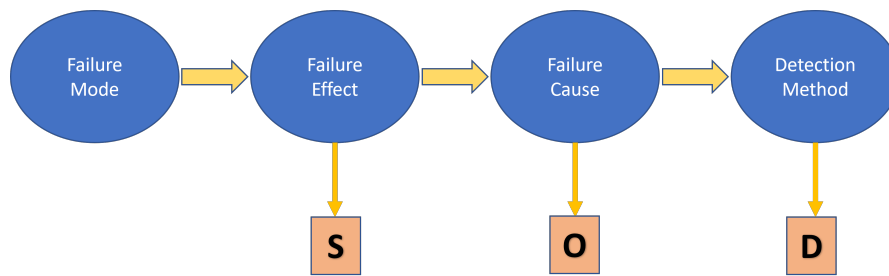


Figure 2.1: Flowchart of FMEA methodology

describes the Recommended actions that are currently performed by the company to correct such failures, Finally presenting the Criticality number and Risk Priority Number.

Name	Function	Failure Modes	Failure effect	S
Cylinder	Pushes the compaction bulkhead	Central Piston Oil Leak	Poor compaction	8
Blade	Compacts waste	Does not return automatically	Control Unit	9
Rail	Sliding compaction bulkhead	Wear of rail runners	Incorrect handling of the compactor	8
			Wear of the rails on which the runners rest	

Table 2.4: First section of SEA FMEA

Analysing Table 2.6 it is possible to see that the most important failure that needs to be addressed is referred to the raking functionality of the blade which is operated by means of two hydraulic cylinders as actuators, such problem presents oil leakage as a failure effect. The second failure in importance is referred to the rails of the system which their functionality is the sliding compaction bulkhead of the cylinders, the cause is the friction between the cylinder rails and the two Teflon wear pads. The third failure case is related to the operation of the cylinders, the failure cause as the previous case is also given by oil leakage.

As seen in the results of FMEA analysis, cylinder leakage is the main problem of this project. Again, may suggest that handmade cylinders could be the main concern of the hydraulic system functioning.

In first place it was mentioned previously that a failure can have more levels, in the presented FMEA the cause of failure in the cylinders was the fluid leakage. For such purpose it was important to have a deeper understanding on how leakages

Failure Cause	O	Failure Detection	D
Oil leaks	7	None	10
Oil leaks	9	None	10
Different friction between the two pistons, different wear of the two pads	8	None	10

Table 2.5: Second section of SEA FMEA

Recommended Action	Criticality	RPN
Replacement of failed components	56	560
Replacement of failed components	81	810
Replacement of failed components	64	640

Table 2.6: Third section of SEA FMEA

occur in hydraulic cylinders, analyze the most common leakage failure causes. With such review it was possible to prepare a possible solution to the problem which will be detailed in later chapters.

In second place the root cause of rail wearing is known by the simple observation that the Teflon also wears, leading to the damage on the rails, thus a solution was be proposed in Chapter 3.

Chapter 3

Failure detection procedures and techniques

In chapter 3 an FMEA analysis of SEA company Farid vehicle was performed, showing the following main root causes of failure modes:

- Oil leakage in both systems i.e., shovel and compaction systems.
- Rail pads wear in the compaction system.

This chapter will analyze in a theoretical way and propose a set of different solutions for the two previously presented failure causes in the SEA hydraulic system.

Before diving into different failure detection techniques it was important to understand the types of maintenance strategies normally used by industries, which are important in order to understand what are the benefits and limitations of the different methods that were later proposed.

3.1 Machine maintenance

Every day a wide range of machines are used in a lot of different areas and for different purposes, due to a continuous use, each machine eventually breaks unless it has a proper maintenance. The idea behind predictive maintenance is to predict when machine failure will occur. This allows the producer to plan machine maintenance in advance, thus make a better usage of his time and maximize the machine useful life. A machine maintenance can be understood in three different strategies:

- **Reactive maintenance:** This refers to use the machine until its physical limits for repairment, i.e., the machine is repaired only when it brakes or fails

due to continuous usage. The main problem arises when the equipment is very expensive and difficult to replace, which will lead to considerable many losses, for very cheap equipment this kind of strategy can work, e.g., a light bulb once it stops working can be replaced easily.

- **Preventive maintenance:** This strategy prevent failure on a basis of a regular and iterative maintenance, which it is established according to some industry specifications. However, there is no estimation of when a failure will occur. As a result, and in order to be conservative, each maintenance planification tend to usually be much earlier than the period when a real failure occurs, especially dealing with critical equipment. This perhaps leads to waste machine working life that could still be usable, eventually increasing costs.
- **Predictive maintenance:** Allows the user to estimate in a time basis when a failure will occur. Having such information will help the producer to plan an optimum maintenance time, thus reduce as much as possible unnecessary costs. Moreover, in many cases predictive maintenance not only detects failures but also gives more detailed information of what component or part of our machine will fail and therefore needs to be fixed.

3.2 Hydraulic systems fault types

It is important to notice that according to and extent bibliographic review [2], [3], in this project more research needs to be done in order to properly implement predictive maintenance in hydraulic cylinders and hydraulic systems in general, however what it is possible to do is to detect leakage failures in a relative early stage, when they do not yet compromise the functionality of the entire system in a higher degree, with such idea it is possible to schedule the required repair.

3.2.1 Oil leakage in hydraulic systems

The important scenarios that have to be analyzed in this document are internal and external leakage in the system. Internal leakage is the unwanted flow which occurs mostly in cylinder pistons across the seal that separates the cylinder chambers, external leakage is defined as unwanted flow out of the system if we take an example from hydraulic cylinders it will happen for the degradation of the dynamic seal system between the rod and the cylinder head. Fluid leakage can cause a reduction in the system force exerted in this case by the cylinders which have to compact the waste and also sustain the shovel in position during the compaction procedure. Since oil in fluid power systems is highly contaminant it can also arise several problems of environmental contamination.

3.2.2 Oil leakage monitoring methods in hydraulic systems

Currently there are no visual features that can be used to monitor initial stages of fluid leakage in hydraulic cylinders until the fluid leakage is either visible or system performance is affected. As it has been seen in the practical analysis of this project and also in literature, fluid leakage ends up affecting dynamic performance of the hydraulic system. This can be visualized mostly in the hydraulic cylinder which in our case are the outcome of the functionality of the entire system. In the last years there has been a more emphasis in the research of signal based techniques for failure identification of fluid leakage.

Detection with tank level measurement sensors Basically it is a common way of detecting leakage in systems, however not quite precise. It consists in installing sensors in the reservoir in order to detect a level variation from the level with no losses, and the level reduced to some degree if there are some leakages in the system. Making a comparison in both cases will lead the user to know if some fluid has been lost by leakage.

Detection with pressure sensors It must be stated that the cutting edge methods are not able to detect fluid leakage before it happens, what they do is to detect them once leakage has occurred. the best methods collect pressure in analog sensors and arrive to detect a leakage of 0.124 L/min of leakage. This will allow the owner to detect the failure before a catastrophic failure occurs if the system continues operating allowing more wear and end eventually to a catastrophic failure where the machine doesn't operate anymore, which is currently, the case of SEA.

According to literature [2], a variety of methods have been used for fluid leakage detection, among them also different types of sensor devices are used to collect data and use different analysis techniques. Most of them are not currently available in the market because further research is needed. On the other hand a signal based analysis measuring the pressure changes using analog pressure sensors have achieved the best results able to detect as mentioned previously a leakage flow of 0.124 L/min. Here we will describe the two most important signal based methods, both of them are based in the decomposition of a nonlinear signal in its different modes i.e., it decomposes the signal into different frequencies in a similar way as the Fourier transform does, however the Fourier transform in general works with LTI (Linear Time Invariant) systems and presents some drawbacks at the time of analysing nonlinear systems, the current methods that will be presented, obtain good performance with nonlinear signal decomposition. The main idea behind them is to detect the change in dynamic behavior of the system, and make a fair comparison between the dynamic behavior in normal operating condition and failure conditions.

In the following subsections different methods that will be used in this document are presented.

Wavelet transform

In wavelet analysis the source signal is decomposed into the time and frequency domains simultaneously. This allows to focus on short time intervals for high frequency components and longtime intervals for low frequency components. An experiment was done by Goharrizi et al. using a wavelet transform to detect fluid leakage. A multi resolution decomposition was used to decompose measured pressure signals into its different modes that is different frequency components. Taking measurement from the device working at normal operating conditions and with oil leakage and estimating the RMS value of both signals. The method was able to detect leakage in the range of 0.2 L/min to 0.25 L/min, [4], [5].

Hilbert-Huang transform

The same author Goharrizi et al [6], was also able to study the Hilbert-Huang transform to detect fluid leakage in the system. The HHT uses empirical mode decomposition (EMD) to decompose the signal into intrinsic mode functions, later the HHT was used to obtain instantaneous frequencies and amplitudes of the signal. In both cases (Wavelet and HHT) the pressure signal obtained from sensors was decomposed allowing further analysis to detect leakages. The proposed technique was able to detect leakages in the range of 0.124 L/min to 0.23 L/min. It has to be pointed out that HHT method obtains more accurate results at the time of detecting leakages, however more computational power is required for that purpose, so in order to implement it into an embedded system for direct online monitoring and leakage detection can be more difficult due to computational power which also leads to more power consumption.

Tank level measurement

For this purpose it can be used pressure sensors which was a first option, however the low amount of such type of sensors for small size reservoirs, like the one this project, and even their very high cost, lead to research for more affordable options.

The best proposition was ultrasonic sensors capable of being installed at the top of the tank and measure the oil level. Two sensors were bought in order to obtain better results from two independent measurements. However a drawback of such proposition is that the measurement can only be done when the vehicle is not moving or in idle position. While the Farid vehicle is at move the oil will also be non stationary as a result of the vehicle movement therefore will give erroneous measurements from the ultrasonic sensors.

3.2.3 Particle contamination in hydraulic systems

It is very important to understand that failure hydraulic systems may be caused by a variety of factors, one of the most important ones is particle contamination, which generates wear due to the friction of small particles and eventually leakage problems in the system. As a result, an analysis into both fluid leakage and oil contamination will be discussed given their mutual dependence.

Fluid contamination and fluid leakage are used as indicators for failure monitoring and predictive maintenance of hydraulic systems. If we take for instance hydraulic cylinders, contaminants in fluid will affect the sliding properties and surface quality of the piston, this will eventually lead to a failure, moreover as a result of failure in surface quality, this will lead to internal and external leakage in the cylinder, giving a similar result of what currently happened to SEA described in the FMEA, which is a reduction of efficiency and power in the system.

Effects of particle contamination

Wear is a common outcome in fluid power components when the system has been continuously used, moreover if a certain component is perhaps not replaced in time it will lead to fluid leakage or contamination of the fluid with particles. Such particles tend to increase the wear of several units that compound the fluid power system. Hard contaminants such as small steel particles are able to cause severe damage to the system. Pollutants are mainly constituted by water, air, dust and small particles steel.

Particle contamination can cause different types of wear such as abrasive wear, adhesive wear, fatigue wear and abrasive wear are responsible for around 90 percent of component failure in hydraulic systems leading the system to different types failures, degradation failure, intermittent failure and catastrophic failure. On the other hand, According to literature [2], in general 65-90 percent of hydraulic system failures are caused by fluid contamination. As a result, it is important a continuous monitoring of oil health in order to maintain it into a regular intervals, this increases the operative life of a given fluid power system. Moreover, explains why all companies perform oil change on a regular basis to their machines as an action of preventive maintenance.

Effects of system overheating

High temperatures are an indicator of particle contamination in the system, this happens mostly when there is an increase in steel debris in the system due to continuous usage or a failure in one of the components. The friction generated by the particles when the system is in operation may cause a system overheat. The changes in temperature in the system also may affect the viscosity of the fluid

reducing it to a point where it may produce leakage in the systems, also since the oil is in charge of lubrication it may also cause more wear in the system for the reduction of effective lubrication in the system.

Heating in fluid power systems is mostly generated for power loss in the different components, an analogy can be made with an electric circuit where the resistors are a source of voltage drop and power loss in the system. In the different types of components of fluid power system due to their own properties, they generate a power loss, and the system losses are converted to heat. The total power lost is equal to the sum of power loss in the different components of the system which are pump, valves, plumbing and actuators.

3.2.4 Particle contamination monitoring methods in hydraulic systems

As it has been seen different degradation features affect fluid quality of hydraulic systems among them we have high temperature, air, water, chemical contaminants, wear debris or dust.

Since we are interested in techniques of detecting failures in the system, it is important to understand what are the most relevant and accessible methods to monitor oil health, for such purpose there exist two methods.

- Direct monitoring methods
- Indirect monitoring methods

Direct monitoring methods are based on visual inspection or geometric measurements, both prioritize the physical change in components. A drawback of direct monitoring methods is that many attempts of performing it such as machine vision or visual inspection have not proven to be economically viable.

Oil health can be monitored by different principles, Physical and chemical monitoring methods which refer to direct monitoring methods, on the other hand electrical (magnetic) and optical refer to indirect methods.

It is necessary to clarify that direct methods are in general difficult to implement and more costly. For instance chemical or physical monitoring require samples of the oil to be analysed in a laboratory, thus as explained before they may be time consuming, moreover it is not possible to implement a real time monitoring. The fact that real time monitoring is not possible yet with direct methods could be in principle one of the major drawbacks such methods could present, given that they cannot be directly installed or implemented as a sensor in a systems that is intended to be analysed. On the other hand for the moment indirect methods are more versatile and capable of real time monitoring, however as the name "indirect" suggests, indirect methods monitor specific properties of the fluid, this depending

on the method that will be implemented and then correlate the acquired data to the fluid condition.

In this document a main focus is given to indirect condition monitoring methods, this is because they are easily implemented on any hydraulic system for real time monitoring.

Electrical (magnetic methods)

Since we have seen that abrasion and surface fatigue are two of the most dangerous effects of particle contamination in hydraulic systems, a part of them derive by metallic debris of the same system due to aging and continuous usage. Bibliography describes a set of sensors from POSEIDON systems which is not only capable of measuring metal debris particles but also non metallic particles as well.

During the inquiries of sensors it was impossible to obtain the required sensor materials from the company, since it has no representative stores in Europe, only in the United States.

Optical methods

Optical methods are one of different forms of oil health monitoring indirect methods, the basic principle is absorption spectroscopy, which correlates the data with the level of degradation of the fluid. they can be permanently mounted on the equipment to measure number of particles and size of particles in real time. Such sensors are available in the market, three clear examples offered by bibliography are the oil particle monitoring from IFM electronics, another one from Bosh Rexroth and also contaminant sensors from HYDAC.

3.3 Teflon rail pads wear fault

3.3.1 Monitoring rail pads Teflon sliders

In order to measure the wear in the rail Teflon pads of the cylinders it was used an inductive sensor, such sensor is able to measure the distance from where it is installed to a position where a metal device is located. Since the Teflon is a plastic material, the inductive sensor measure through the Teflon to the rail where the Teflon pad slides. As a result it is possible to measure the Teflon pad wear by the distance of the sensor and the rails

3.3.2 Misalignment of the cylinders

In the worst case scenario, when the Teflon pad is completely worn, there exist a misalignment with the two cylinders that push the shovel for waste compaction.

This is due to an increase of friction forces of the only metal contact in this case between rails and sliding pads. As a result a last resource to detect this misalignment is by two accelerometers, each one installed on each one of the two cylinders in charge of the compaction process. As a result a change in the displacement may lead to a detection of possible failure, before a catastrophic damage is done to the system.

3.4 Description of sensors

Since the required sensors have been described, their locations into the hydraulic system are shown in Figure 3.1, here it is possible to see where will be the sensors installed in the hydraulic system in order to acquire the necessary data for analysis.

3.4.1 Pressure sensors

Type of sensor

The selected sensor is the IFM PT5501. See Figure 3.2.

Main characteristics

- Range of measurement: 0 to 250 bar.
- Operation temperature: -40 to 125 °C.
- Pressure range tolerance: Up to 625 bar.
- Power supply: 8 to 32 V.
- Output signal: Analog signal 4 to 20 mA .

Installation on the system

Two PT5501 IFM pressure sensors were installed close to the circuit corresponding to the inlet flow to the cylinder which is in charge of the compaction of the waste, therefore aligned with the highest pressures. See figure 3.3

3.4.2 Temperature sensors

Type of sensor

The selected sensor is the IFM TA3105. See Figure 3.4.

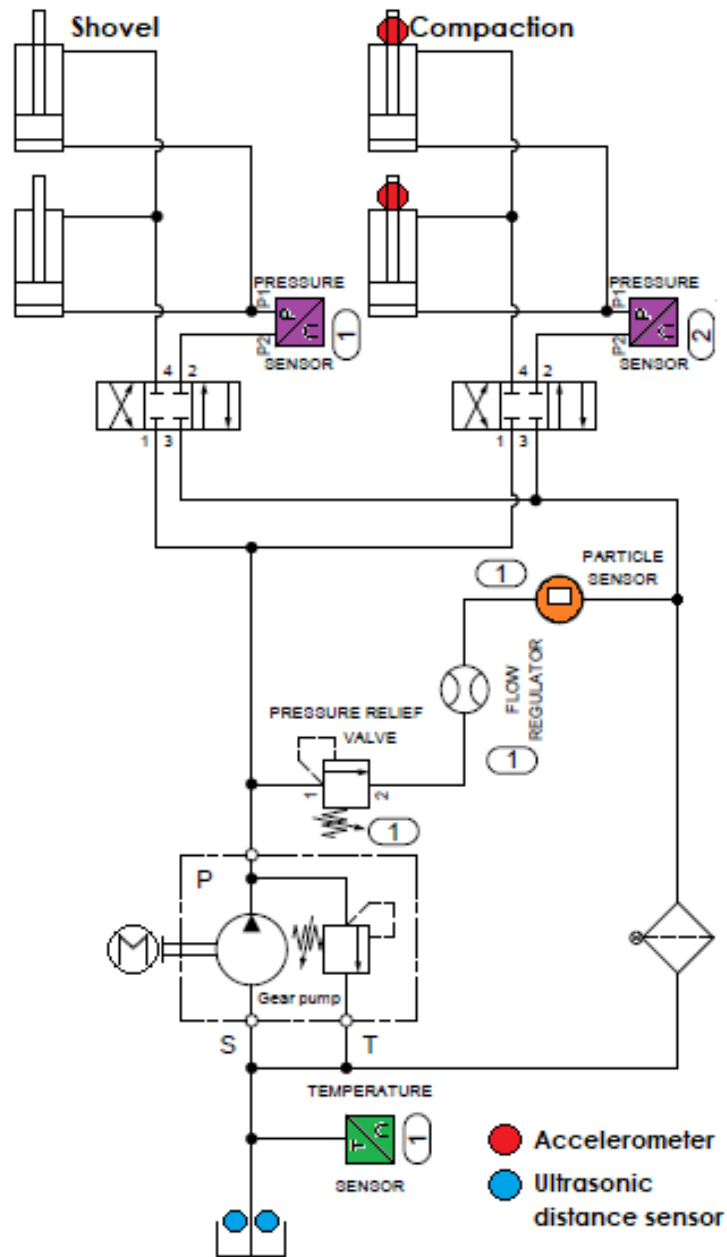


Figure 3.1: Hydraulic system schematic with sensors

Main characteristics

- Range of measurement: -50 to 150 °C.
- Pressure range tolerance: Up to 400 bar.



Figure 3.2: PT5501 IFM pressure sensor

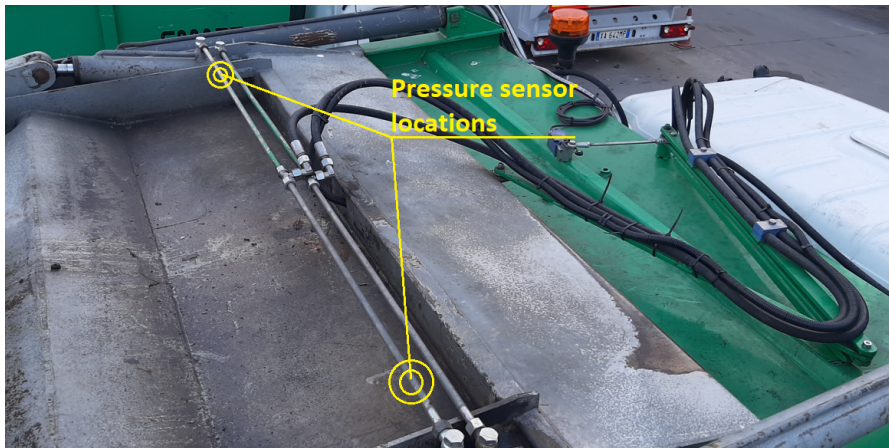


Figure 3.3: Locations of installation of pressure sensor in the system

- Power supply: 10 to 30 V.
- Output signal: 4 to 20 mA.

Installation on the system

One TA310 IFM temperature sensor was installed in the lower section of the reservoir. A hole was drilled and through the thread of the sensor the installation was carried out. See Figure 3.6.



Figure 3.4: TA310 IFM temperature monitor

3.4.3 Oil level monitoring sensor

Type of sensor

The selected sensor is the Microsonic mic+25/IU/TC. See Figure 3.5.



Figure 3.5: mic+25/IU/TC Microsonic Ultrasonic distance measure sensor

Main characteristics

- Range of measurement: 30 to 350 mm.
- Temperature tolerance: -25 to 70 °C.
- Power supply: 9 to 30 V.
- Output signal: 4 to 20 mA.

Installation on the system

Two mic+25/IU/TC Microsonic Ultrasonic distance measure sensors were installed in the upper section of the reservoir. A hole was drilled and through the thread

of the sensor the installation was carried out, this will allow to measure the fluid level. See Figure 3.6



Figure 3.6: Oil level sensors location

3.4.4 Oil health monitoring sensor

Type of sensor

The selected sensor is the IFM LPD100. See Figure 3.7. The optical IFM LDP100 sensor was selected and acquired. Its functionality relies the principle of light extinction to operate. The sensor is compounded by basically three elements, a measurement cell, a laser beam generator and a photo diode. As a particle passes through the laser beam, the light in intensity detected by the photo diode is reduced, the large is the particle the larger the reduction of light intensity. This allows to make a correlation of the size and amount of particles by the sensor. At the end the particles are classified with regard to their size and number, the measured value is provided according to ISO 4406:99 or SAE AS4059R, which both are typical measurements that indicate the level of fluid contamination in our system, this provide useful information about the state of health of oil in the system.

Main characteristics

- Range of measurement: 4 to 21 μ -meters particle size detection
- Operation temperature: -10 to 80 °C
- Pressure range tolerance: Up to 420 bar.



Figure 3.7: LDP100 IFM optical particle monitor

- Power supply: 9 to 33 V.
- Output signal: 4 to 20 mA.

Installation on the system

This sensor has to be installed after the pump with a flow regulation and pressure regulation valve in order to maintain the fluid flow into a certain threshold for better results. This is specified in the data sheet and such procedure has been done for the current project. See Figure 3.8



Figure 3.8: C optical sensor installation

3.4.5 Accelerometer for cylinder misalignment

Type of sensor

For this case the ST, STEVAL-STWINKT1B board is used. See Figure 3.9. This boards no only contains an accelerometer, it also contains a humidity sensor, a temperature sensor, ultrasonic sensor, moreover it also has a predictive maintenance firmware able to detect variations in acceleration measurements and therefore identify some damages of the system.



Figure 3.9: ST, STEVAL-STWINKT1B board

Main characteristics

- Operation temperature: Since the board has many sensor what the weakest range was taken among all of them which is from -40 to 85 °C. For more information the data sheet of the sensor can be reviewed.
- Power supply: 5 V.
- Output signal: Analog or digital output voltage

Installation on the system

The STEVAL-STWINKT1B boards are installed in the shovel in order to be able to measure its movement.

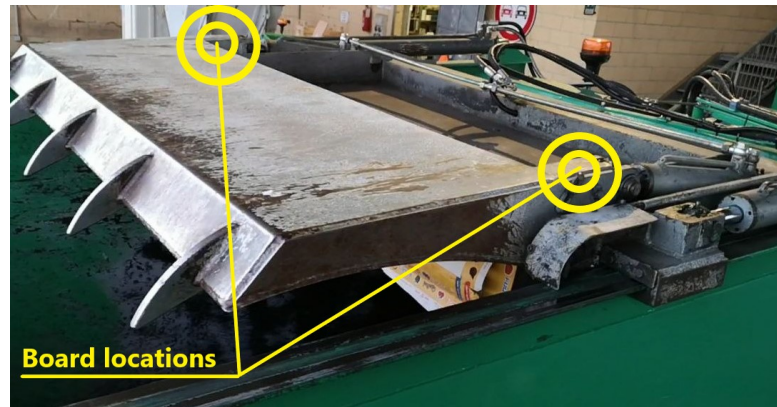


Figure 3.10: STEVAL-STWINKT1B board location in the system

3.4.6 Teflon sliders wear sensors

Type of sensor

The selected sensor is the Contrinex DW-Ax-509-M18-320 inductive sensor. See Figure 3.11



Figure 3.11: Contrinex DW-Ax-509-M18-320 inductive sensor

Main characteristics

- Range of measurement: 10 mm.
- Operation temperature: -5 to 70 °C
- Temperature drift: <5% (0 to 70 °C), <10% (-25 to 0 °C)
- Power supply: 15to 30 V.

- Output signal: 4 to 20 mA.

Installation on the system

The inductive sensor is installed by drilling a hole on the top of the sliding pad section. See Figure 3.12



Figure 3.12: Inductive sensor position

Chapter 4

Data acquisition system

The data acquisition system was designed and built in order to implement it to the targeted hydraulic system. Given its complexity such project counted with the help of an engineer that the CIM 4.0 provided in order to develop due to its technical complications. In this chapter it will be described the system and its functionality in a general purpose.

Arduino Mega 2560

As an overall idea the data acquisition system possesses the sensors described in the previous chapter, the data is processed by an Arduino Mega 2560 board it is presented in Figure 4.1 , this is a microcontroller based on ATmega2560. It has 54 digital input/output pins, 16 analog inputs, 4 UARTs (hardware serial ports), a 16 MHz crystal oscillator, a USB connection, a power jack, an ICSP header, and a reset button.

The purpose of the Arduino Microcontroller is to process the data of the Oil health sensor LDP100, the pressure sensors PT5501, the ultrasonic reservoir oil level monitoring sensors mic+25/IU/TC and the temperature sensors TA3105, it also has to receives the binary signals from the truck system. Once some binary signal is activated the Arduino immediately will start collecting data from the sensors of the system that is functioning.

Raspberry Pi 4

Since the data that will be collected by the accelerometer will be at a very high sampling rate, a lot of data needs to be processed, the 16 MHz at which the Arduino functions was not enough, for this reason a Raspberry Pi board was used, Figure 4.2. The Raspberry Pi is basically a single board computer. It has all the same components of a desktop PC, but in a much smaller form factor, here only the

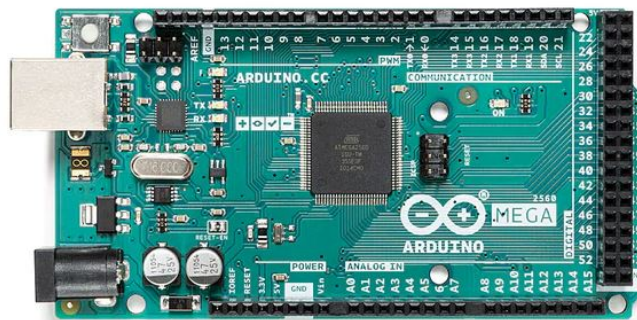


Figure 4.1: Arduino Mega 2560 board

necessary characteristics useful for this project are described, for more information it is advisable to search online documentation. The Raspberry Pi 4 can reach a 4 BG RAM. It has a Quad core 64-bit ARM-Cortex A72 running at 1.5GHz this allows also a faster data processing. Depending on the model it has a 1, 2 and 4 Gigabyte LPDDR4 RAM .Among the interfaces it has a 802.11 b/g/n/ac Wireless LAN which uses dual-band wireless technology, supporting simultaneous connections on both 2.4 GHz and 5 GHz Wi-Fi devices, it has one SD Card, two micro-HDMI ports, two USB2 ports, two USB3 ports, one Gigabit Ethernet port (supports PoE with add-on PoE HAT), 28 user GPIO supporting various interface options:

- Up to 6x UART
- Up to 6x I2C
- Up to 5x SPI
- 1x SDIO interface
- Up to 2x PWM channels
- Up to 3x GPCLK outputs

The main purpose of the Raspberry Pi 4, due to it's high data processing was for processing mainly the accelerometer data, moreover receive all the data processed from the Arduino board and send the sensors measured data it in real time via WiFi connectivity to a cloud for later processing.

4.1 High level description of the system

Figure 4.3 shows an overview of the data acquisition system, in brief each component functionality is described.



Figure 4.2: Raspberry Pi 4

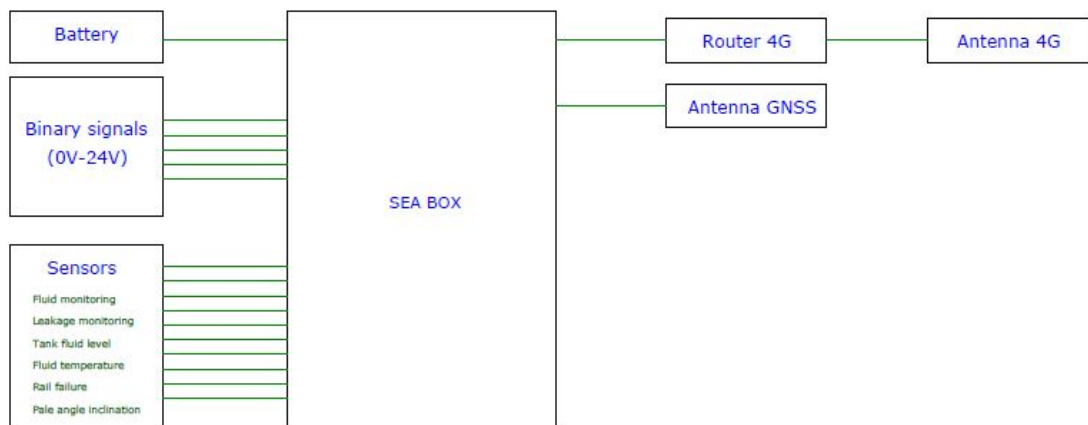


Figure 4.3: General schematic data acquisition system

- Battery: The battery just the car battery of 24 V. which make the whole system work. Inside it contains the power distribution supply module which was discussed later in this chapter, basically this module turns ON the system when the car is also turned ON, and turns OFF when it has finished sending all the collected data.
- Binary signals: The garbage collective trucks have embedded different types of systems, for instance the hydraulic system that compress the garbage is one of them, the hydraulic system that picks up the garbage boxes from the street is another one. For this reason and in order to control each one of them from a control panel, binary signals are used in order to activate or deactivate a certain system for a required amount of time.

- Sensors: This box contains each one of the sensors selected by the system that will collect the data
- SEA box: This box contains an Arduino board and a Raspberry Pi, both of them are used for the purpose of processing the data collected by the sensors. The Arduino will collect the data which did not require a very high rate sampling, on the other hand the Raspberry pi purpose was to process the high amount of data collected by the accelerometers which were able take very high rate sample time. It also contains other systems that will be described in brief
 - Power supply and power distribution system
 - Signal conditioning module
 - Sensor modules
 - GNSS module
- Router 4G: The router purpose was to connect to Internet with a SIM card, the idea was to send the data in real time independently of the truck's position. Such router signal was also incremented for a much better performance with an antenna 4G, thus the performance was maximized.
- Antenna GNSS: The purpose of a GNSS or a GPS antenna is to track the truck's position in real time.

4.2 SEA Box description

As mentioned previously the SEA box contains a set of different modules that are part of the data acquisition system, next in this chapter, the different circuits part of the system hardware were described and the design criteria behind each one.

4.2.1 Signal conditioning module

As previously mentioned the garbage truck has different types of systems, each one of them operated with different binary signals that send the commands in order to activate or deactivate certain actuators for required operations. The binary signals are the following:

- KEY: Indicates whether the vehicle key has been turned, so at least the vehicle panel is switched on.
- EV_CHIUSURA_PALA: Indicates whether the solenoid valve that closes the blade to collect waste is active.

- EV_APERTURA_PALA: Indicates whether the solenoid valve that makes the blade open to stop collecting waste is active.
- EV_DISCESA_SLITTA: Indicates whether the solenoid valve that moves the blade to the non-compaction position is active.
- EV_SALITA_SLITTA: Indicates whether the solenoid valve that moves the blade up to the maximum compaction position is active.
- PROX_PALA_APERTA: Indicates whether the blade aperture proximity sensor is active
- PROX_PALA_CHIUSA: Indicates whether the blade closure proximity sensor is active
- FINEC_SLITTA_BASSA: Indicates whether the low blade limit switch sensor is active
- FINEC_SLITTA_ALTA: Indicates whether the high-blade limit switch sensor is active
- MESSA_IN_SCARICO: Indicates whether the discharge has been enabled, then the use of oil for the pistons
- EV_SALITA_AVC: Indicates whether the solenoid valve that raises the container lift is active.
- EV_DISCESA_AVC: Indicates whether the solenoid valve that lowers the container lift-vault is active.
- EV_SALITA_VASCA: Indicates whether the solenoid valve that raises the tank is active.
- EV_DISCESA_VASCA: Indicates whether the solenoid valve that lowers the tank is active.
- EV_PIED_APERTURA: Indicates whether the solenoid valve that places the feet is active
- EV_PIED_CHIUSURA: Indicates whether the solenoid valve retracting the feet is active

These signals have been adapted in voltage so that, considering an input voltage range from 0 to 28V, they have an output voltage range from 0 to 2.56V. This was done so that they can be read by the Arduino ADC, which has been configured with a reference voltage of 2.56V. The signals passed through a multiplexer that

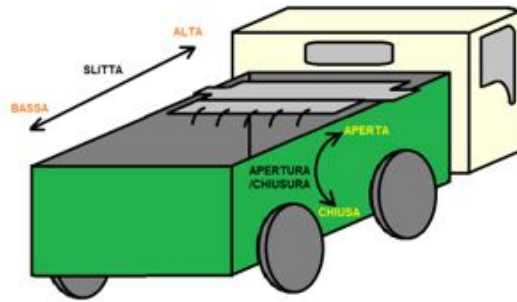


Figure 4.4: Truck binary signals representation

allowed to use a single ADC input of the Arduino to read them all. On the firmware side, a smith trigger filter has been implemented that considers a logical "0" only the voltages below 10V and a logical "1" only those above 20V. Voltage variations between 10 and 20V did not change the logical state of the signal on the Arduino Firmware. Variations of binary signals were saved.

4.2.2 Power supply and power distribution system

Power supply system

In Figure 4.5 it is possible to see the system. As it is possible to observe the component "U1" is a power switch which basically works as a relay that let pass the power from "VBB" to "OUT" in the case that the "IN" pin is connected to ground GND. When the vehicle was turned on, the "KEY" signal had 24 V, this made the Voltage of the Q1 obtaining a voltage divider of R1 and R2, this gave a final voltage value of 4.65 V, the MOSFET Q1 goes from being opened to be closed when the voltage is higher than 2.1 Volts (such value was available on the MOSFET datasheet 2N7002 as V_{GSth}), for such reason if "KEY" is equal to 24 Volts the value of $V_{GS} = 4.65$ V and Q1 will close.

When Q1 goes to closed, it connects IN and GND, and for such reason U1 connects VBAT (24 V) in its output, giving power to PS1 which is a DC-DC converter that outputs 5 V from 24 V.

As previously mentioned 5 Volts power the Arduino which turns on and executes the firmware code that in its set up, initializes the SLEEP_PIN and KEY_PIN, which are the SLEEP and KEY_5 pins that are seen in the schematic of figure 4.5. In the firmware the SLEEP_PIN was configured as an output and is set to HIGH (Arduino sets 5V into that pin), in such a way that the transistor Q2 will close (because $5V > V_{GSth} = 2.1$ V). Therefore in this case, it is the Arduino the one that guarantees that the switch U1 is available and power flows through the

Oil monitoring sensor module LDP100

The oil monitoring sensor is a linear sensor, it has a single analog output but sequential in time. Which means that it allows the user to get four measurements on the same analog channel, but the reading of the signal had to be triggered using the synchronization signal (1) see Figure 4.6. The time between readings is 60 seconds

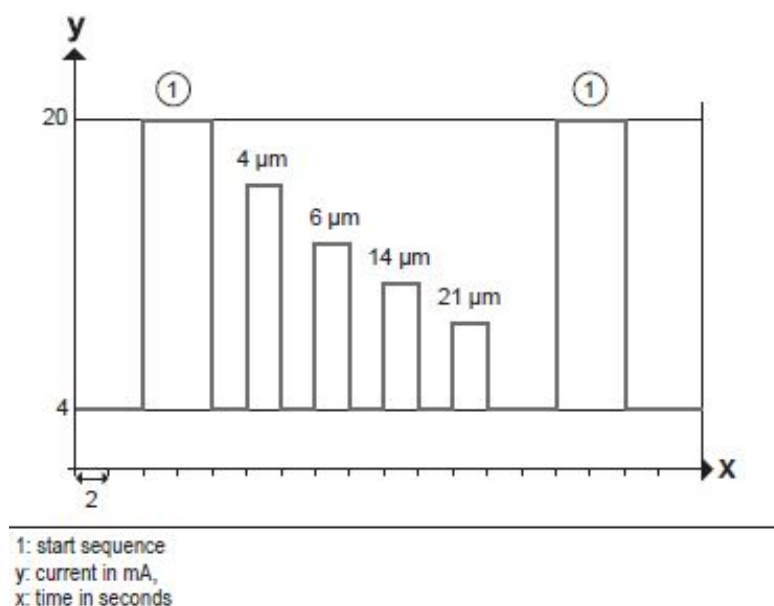


Figure 4.6: Sequential data output via the analogue output

According to figure 4.7, the sensor has a connection of 8 pins.

- The first and second pins are basically referred to the voltage input from the battery with the positive and negative terminals
- The third and fourth pin are the CAN protocol communication which are not used.
- pin 5 is a sensor input which basically gives the sensor the order to start measuring
- pin 6 is the output measurement from the sensor in the range of 0 to 20 mA.
- pin 7 is another output corresponding to the alarm in order to tell the user when the measurements have surpassed the maximum allowed in ISO 11943. Such pin will not be used in our project.
- the pin 8 correspond to ground.

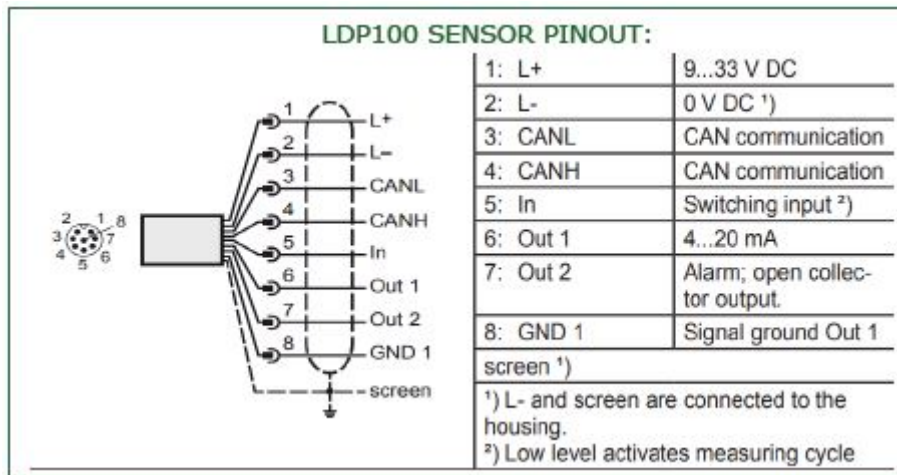


Figure 4.7: LDP100 sensor pinouts

Figure 4.8 shows the circuit schematic of the LDP100 sensor as we can see the LDP100_INPUT where also has the same criteria of closing the mosfet in order to activate such pin. is the LDP100_OUTPUT measured with the 100Ω resistance and LDP100_ALARM which was not be used.

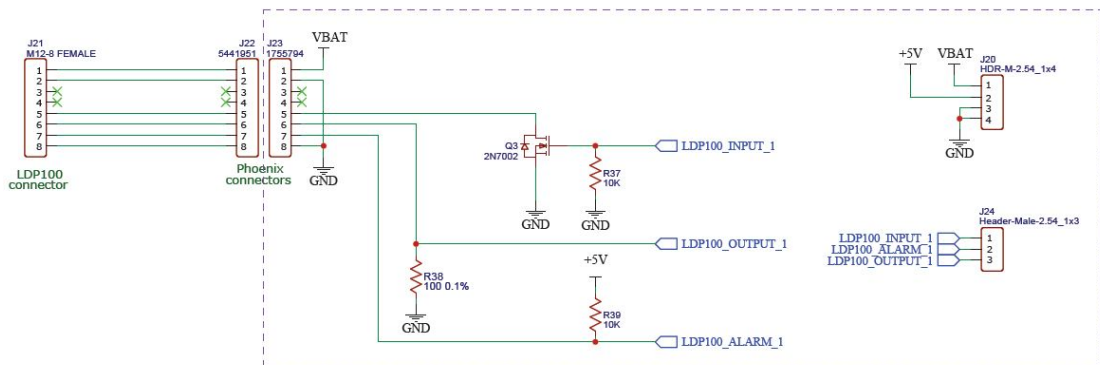


Figure 4.8: LDP100 circuit schematic

Pressure sensors module PT5501

The pressure sensors are also Linear ones, The time between readings: 10 seconds default, 10ms when hydraulic system was used, this means when the system was under operation.

The linear formula to obtain the measurement conversion is the following:

$$Pressure(bar) = 15.625 * Current - 62.5$$

The principle used was quite similar as the mentioned before, this means that the measurement were collected as a current, then a resistance of 100Ω was used to have the measurements as voltage values. See Figure 4.9

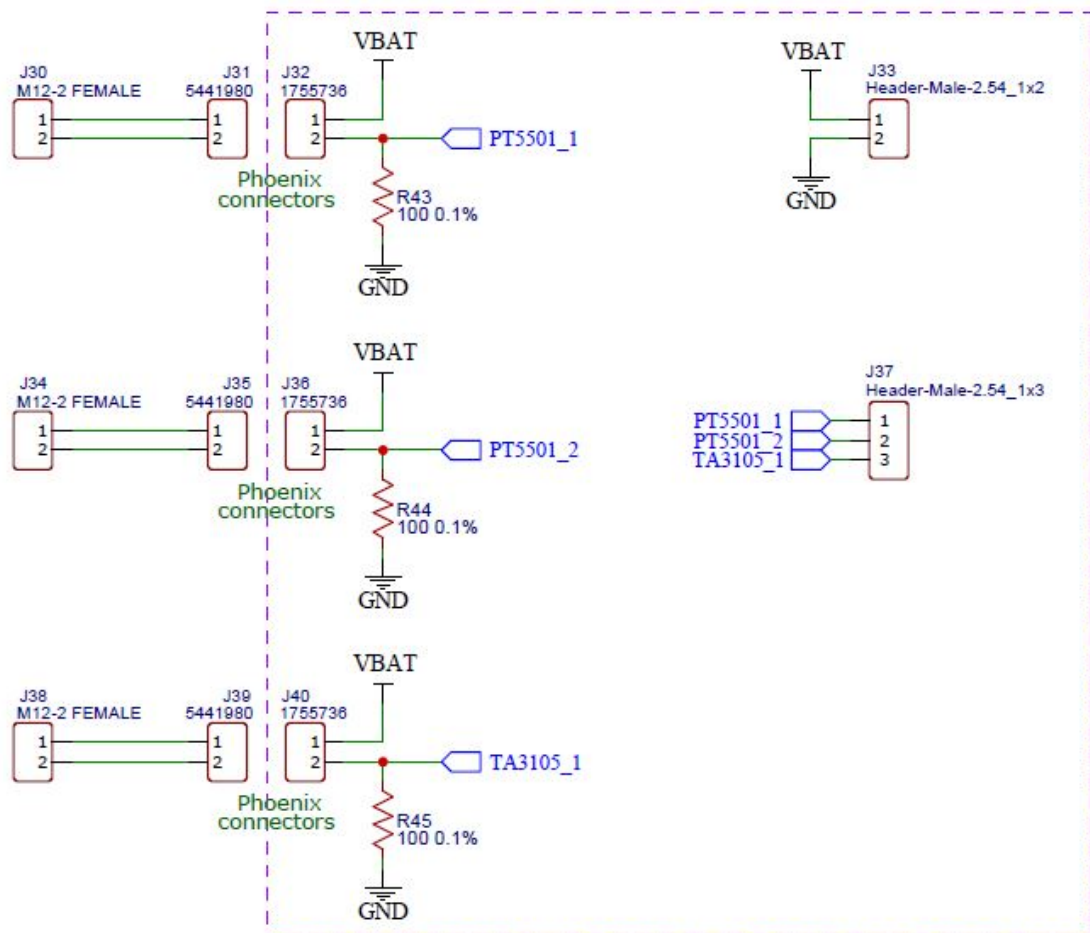


Figure 4.9: PT5501 and TA3105 circuit

The pressure sensors have two pins, the first one refers to the power that was given to the sensor, and the second collected the measured data as a current.

Temperature sensors module TA3105

The temperature sensor is also a linear sensor. The time between readings was 10 seconds and the conversion formula is the following:

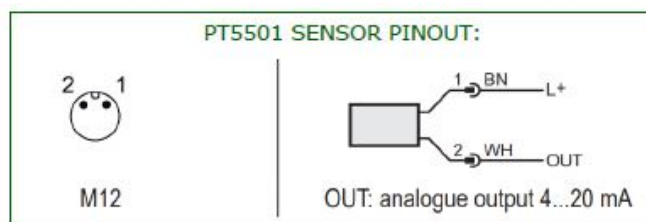


Figure 4.10: pressure sensor pinout

$$Temperature(^{\circ}C) = 12.5 * Current - 100$$

The pin configuration was exactly the same as the pressure sensors

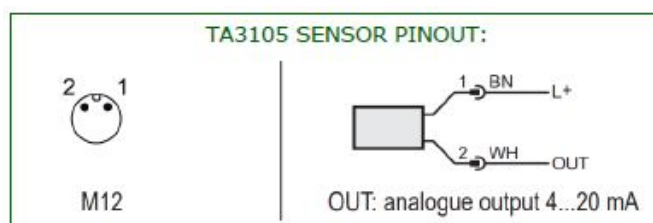


Figure 4.11: Temperature sensors pinout

Ultrasonic sensor module mic+25/IU/TC

This is also a linear sensor, with saturations at the end of the permissible ranges See Figure 4.13. The time between readings was 10 seconds. The conversion formula is the following:

$$Distance(mm) = 13.75 * Current - 25$$

As previously mentioned, two sensors at each corner of the reservoir have been installed, the measurement principle is the same as before with the resistance in order to obtain a voltage from the current given by the sensor measurement.

Inductive sensors module DW-AS-509-M18-320

The inductive sensor was the only nonlinear sensor that was used in the system, in order to obtain a good conversion it was used a fifth-degree polynomial approximation of its response diagram for steel, which is the material of the guide where the skate displaced. The time between readings was 10 seconds.

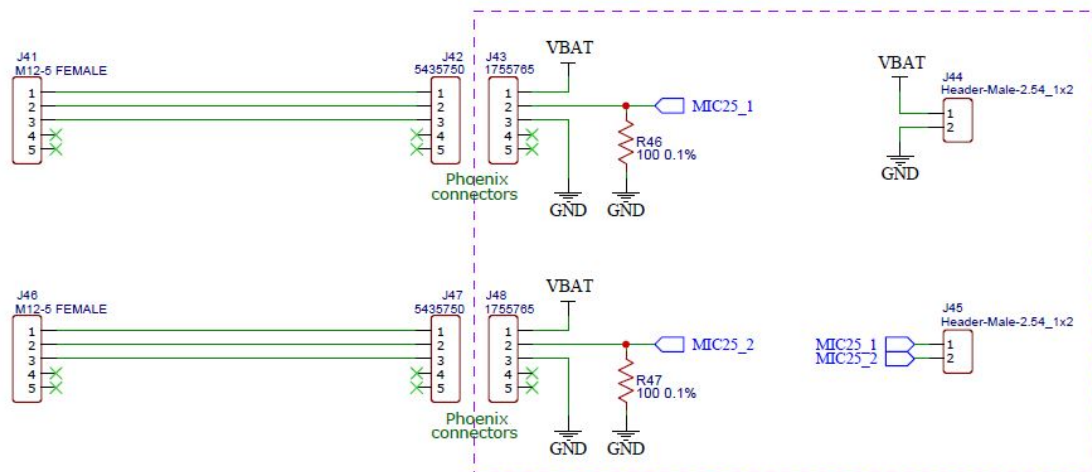


Figure 4.12: mic+25/IU/TC circuit schematic

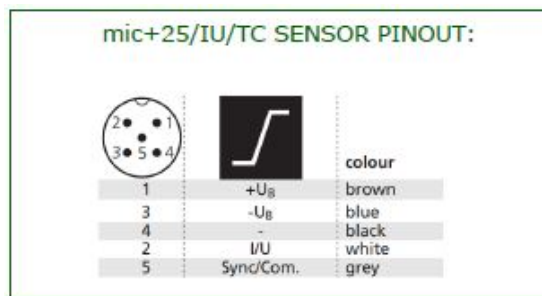


Figure 4.13: mic+25/IU/TC sensor pinouts

$$Distance(mm) = a*current^5 + b*current^4 + c*current^3 + d*current^2 + e*current + f$$

where:

$$a = 0.0001322917461$$

$$b = -0.007924966896$$

$$c = 0.1862139936$$

$$d = - 2.131653828$$

$$e = 12.1981931$$

$$f = - 24.68782882$$

All analog sensors are read by the Arduino, for which the reading times of each sensor were set through a serial communication of the Raspberry with the Arduino. The default times were set as soon as the communication port was opened between the Raspberry and the Arduino. Instead, when the hydraulic system was used, a

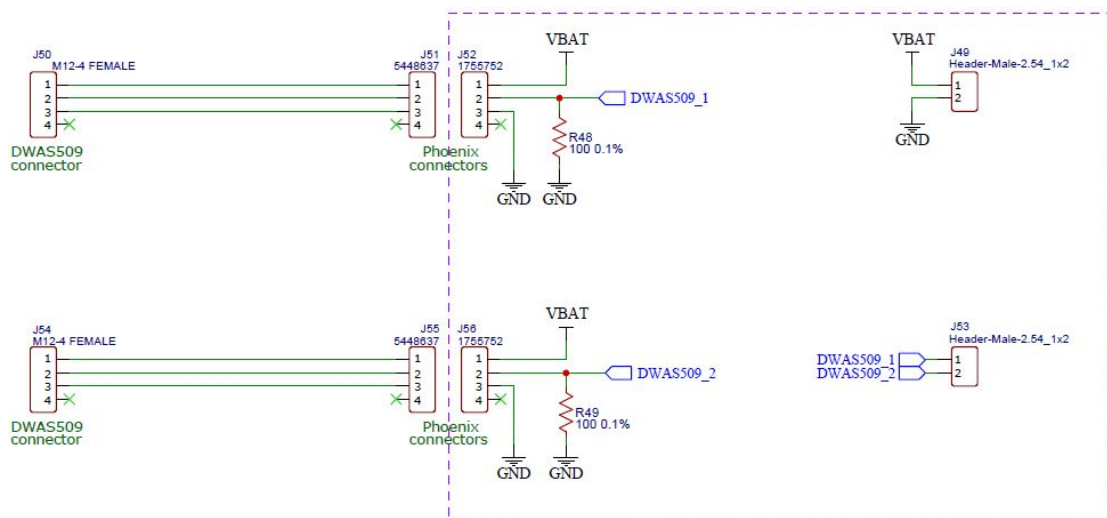


Figure 4.14: DW-AS-509-M18-320 circuit schematic

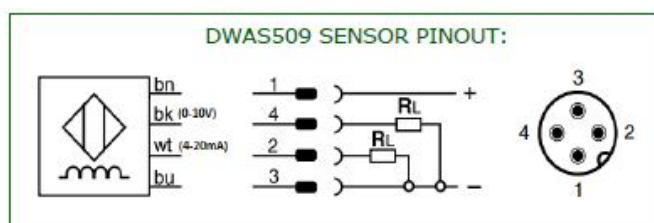


Figure 4.15: inductive sensor pinout

faster measurement time of the system pressure was settled. Similarly, the data sent from the two ST boxes was only saved when the blade for waste compression was being used. In order to know when the the shovel was used or not or any other system that was functioning, binary signal were used.

4.2.4 Accelerometer box STWINKT1B

The board, together with a dedicated electronics, has been locked in an IP68 box in order to make it waterproof. See Figure 4.16

An M12 connector of 8 pins allowed both to bring power and communication with RS232 interface. The system was called for simplicity ST box.

The DC-DC converter allowed to have an input power range from 9 to 36V, so as to be compatible with the vehicle battery (24V).

Instead, the RS232-TTL level shifter made possible to convert the TTL 5V serial signals of the STEVAL STWINKT1B into signals with RS232 levels, which

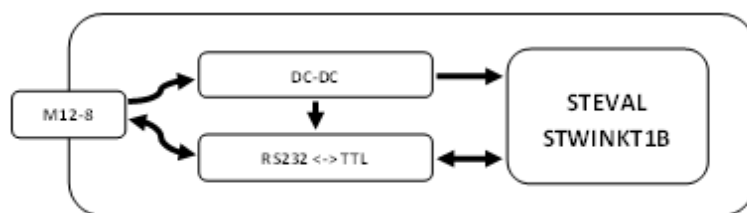


Figure 4.16: Accelerometer installation

contributed to have fewer losses and therefore was able to communicate over longer distances.

4.2.5 4G GNSS module

GNSS

A SIM7600X module connected to the Raspberry was used as GNSS to have the location of the vehicle in real time.

RTC

A Real Time Clock (DS1307) was added, connected to the Arduino, in order to have a time reference for sensor readings. The RTC value was read each time the system was switched on and was updated using the date and time obtained from the GNSS only if there was a misalignment between them of more than 10 seconds.

Router 4G

A KuWFi CPF905 router was chosen to achieve internet connectivity, see Figure 4.18

The router was placed outside the BOX of the SEA BOX, but fixed to the side. All inside the cab of the vehicle, so protected from the weather.

4.2.6 Data processing

As mentioned previously, once the Raspberry operating system started up, a script was automatically executed. The script established communication with the Arduino and set the default reading times of each of the analog sensors. The Arduino read the sensors with the settled times and will asynchronously transmit the readings to the Raspberry. The variations of the binary signals were also detected by the Arduino and transmitted asynchronously to the Raspberry. The Raspberry also opened the serial ports of the two ST boxes, but did not listen to

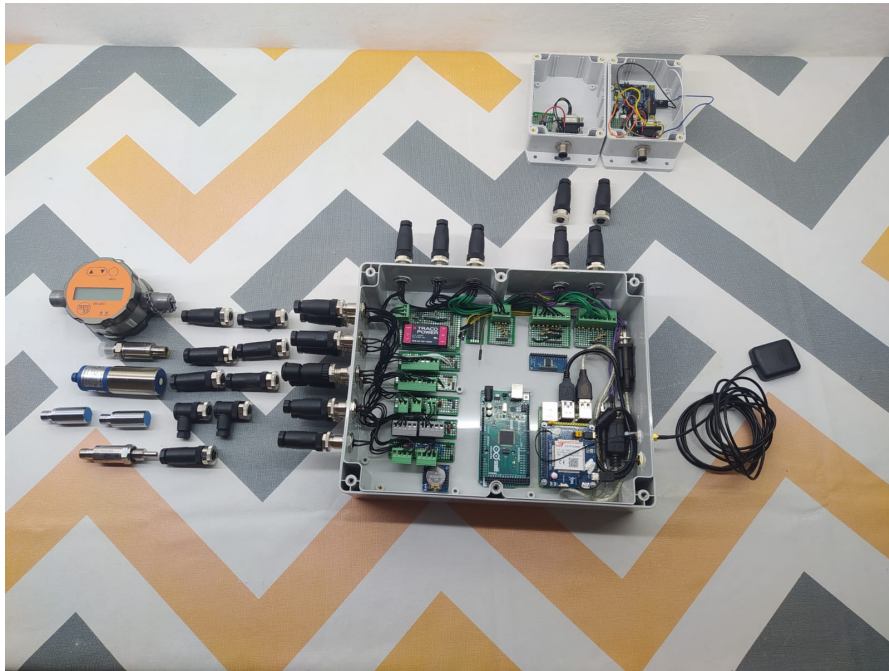


Figure 4.17: Final data acquisition system

them until the hydraulic system is in use. The Raspberry establishes communication with the GNSS module and the positioning data was read periodically. To have a time log, the date and time of the operating system was used, which was set at each power on, through the RTC of the system. All this information processed by the Raspberry was logged into a text file with a certain protocol.

4.2.7 Log protocol

The first column is the vehicle ID.

The second column is the log counter, which increments for each log row added and resets with each new ignition of the vehicle/system.

The third column is the timestamp in Unix Epoch time.

The fourth column is an identifier of the type of information that is logging in:

- INFO = 1: Info system
- SIGNALS = 2: Binary signals
- GPS = 3: GPS
- ST1 = 4: Accelerometer 1



Figure 4.18: KuWiFi CPF905 router

- ST2 = 5: Accelerometer 2
- LDP100 = 6: Oil Quality Sensors
- PT5501 = 7: Pressure sensors
- MIC25 = 8: Oil level sensors
- TA3105 = 9: Temperature sensors
- DWAS509 = 10: Skate wear sensors

Info system

The following messages can be logged in the next column:

- VEHICLE FAR FROM THE BASE: Indicates that the vehicle has moved away from SEA by more than 500 meters
- VEHICLE NEAR TO THE BASE: Indicates that the vehicle has re-entered a range of 500 meters from SEA

- DATE AND TIME SYNCHRONIZATION: Indicates a re-synchronization of the system's RTC, which happened if the system date/time differs by more than 10 seconds from the date/time detected by GPS.

Examples:

1;1;1642310316.316292;1; VEHICLE_FAR_FROM_THE_BASE
1;2;1642310326.316292;1; VEHICLE_NEAR_TO_THE_BASE
1;3;1642310336.316292;1;DATE_AND_TIME_SYNCHRONIZATION

Signals

The fifth column indicates the amount of signals and the next columns, the status of each binary signal (1:HIGH, 0:LOW). There are 16 binary signals and they are as follows (in order):

- KEY = 1
- EV_CHIUSURA_PALA = 2
- EV_APERTURA_PALA = 3
- EV_DISCESA_SLITTA = 4
- EV_SALITA_SLITTA = 5
- EV_SALITA_AVC = 6
- EV_DISCESA_AVC = 7
- EV_SALITA_VASCA = 8
- EV_DISCESA_VASCA = 9
- EV_PIEDINI_APERTURA = 10
- EV_PIEDINI_CHIUSURA = 11
- PROXIMITY_PALA_APERTA = 12
- PROXIMITY_PALA_CHIUSA = 13
- FINECORSO_SLITTA_BASSA = 14
- FINECORSO_SLITTA_ALTA = 15
- MESSA_IN_SCARICO = 16

Example:

1;1;1642310316.316292;2;16;1;0;0;0;0;0;0;0;0;0;0;0;1;1; Tall signals at the bottom except KEY, FINECORSO_SLITTA_ALTA and MESSA_IN_SCARICO

GPS

From the fifth column onwards:

- Latitude (ddmm.mmmmmm)
- N/S (N=north, S= south)
- Longitude (dddmm.mmmmmm)
- E/W (E=east, W=West)
- Data (ddmmyy)
- UTC time (hhmmss.s)
- Altitude (meters)
- Speed (knots)
- Course (degrees)
- Time (0)

If the system does not yet have the info from the GPS available, it logs in empty columns

ST1 and ST2

As described above in the communication protocol of the ST box, from the fifth column and forward, the data arrived first in time and then in the next three lines, the data arrived in the frequency spectrum.

Example:

LDP100

The fifth column indicates the amount of sensors of that type, the sixth indicates the index of the sensor that is logging in at that time and the next 4 columns indicate the Range Number values (from 0 to 26) for particles of 4um, 6um, 14um and 21um respectively.

Example:

1;1;1642310366.316292;6;2;1;12;10;8;6

OZ (4um) = 12

OZ (6um) = 10

OZ (14um) = 8

OZ (21um) = 6

```

1;1751;1652785990.969191;4; TIME;4G;-584;-2345;7110;924;-105;10465

1;1753;1652785991.021433;4; FFTX;
006CFFB3B3AEB8C8B8B5AEB5A2B1B3AEACA2BAB39BBABABCC3C1C6C8D2D4EEF0D4D2C8BAC69BC1ACB8A0ACB3AEB8A0ACA5AEA
A8BAE97ACAEA2B8A7B1BAE0BCC1B1B5B5CBBCA79B97B1AE81A0BAACA7AAB1BFA7AEB8ACA7B3BAB8B1BACDA7B5AC9BAEC8BCA2ACB
CBABAA5BCB3ACC6B1B5B8BCB8B8B3B184A299A284AA0A592A2A7AEA2AAB3A0B199A59992A29EAC8D9297AE9EA5AE8488ACB3AEB5
ACA0A2A2B5A797AA92AEB3AEA5B1A2B1ACA7A2A0AE94B19EA5B1A5ACAEAAAAAACB3A0AE94AE97AAB1A2A5AE94A0B3AEA0A0A592
AAAAAAAAA2AAA7ACA0A0A5AA9997AC84AAA0A2A29EA59E97A099A5ACA792A7A7A2A09BAA97ACAEA 2A2999B9B90A7A2A551

1;1758;1652785991.073654;4; FFTY;
007AFFA5B19CC0C6D3D5C6B3B3B1AFB1AF9AA99CA5A5A79EA5ABB5A9ABAFBEC4D7D9C2B87B3B7B19EAB9AA0A9B1AFA3A3A59C90B
790A39EA9A0A9A081A39CB598A99E9894ABABA59A9A9A949C9A908EA0A08C989A9692A990A59EAF9CABB8C99A8196A5AD9A948E9E9
892988E96A0AB98929E9287A3A970A07FA0A3AFA381A3989C8C9489949A9C929687899C728E89899489949492948E81859E7B7B898
C90A0909E8E92988E839E79A39483879A85908E778E8E90909C928C92988183908C758C94879694927796927FA372897292908E929292
8E94909A9889968C948E6C90898C799A8E878C7F6694969079949081878E85909A7D927 992858C9090949A858E

1;1761;1652785991.125949;4; FFTZ;
008BFF7A8B96949DAEB09F96968294A577877C928492218D8B96988D6A9AA19DA685AA9A8D967AA37E908F8B84889685828D8D7782
9080848FA59F879492A1C4989A9D908FA59D827C8D8F9085969A90879DA6AC80969AA89DB3949D9DB5C2A3AAA196A3AA9690989AA3
9F98858D9B8F9880989B9AA3A6A19F988882969498968D8D969A89988589908B8098878F94928F7E9887829485877C897C8D85798B7A
89967E8580858487848D849275848B807C907980897A7E797980648D8D7C668B927E878D8289848287778F8B8580808985888B87A7A
77877A777A7980826C7780778279778277898F7E778582898771857E717E80888D68808 571805D75876E7A8491

```

Figure 4.19: Accelerometers collected data

PT5501, MIC25, TA3105, DWAS509

The fifth column indicates the amount of sensors of that type, and the next ones indicate the respective measurements of each sensor.

Examples:

- **PT5501**
1;1;1642310366.316292;7;2;10.25;50.12
PT5501_1 = 10.25 bar
PT5501_2 = 50.12 bar
- **MIC25**
1;2;1642310366.418741;8;2;45;65
MIC25_1 = 45 mm
MIC25_2 = 65 mm
- **TA3105**
1;3;1642310366.471703;9;1;32
TA3105 = 32 °C
- **DWAS509**
1;4;1642310366.578607;10;2;3.25;4.32

DWAS509_1 = 3.25 mm

DWAS509_2 = 4.32 mm

4.2.8 Saving Data

Logged-in data is saved locally in real time to a text file with a .log extension. All log files of different date to the current date of the system are uploaded to a cloud for its subsequent predictive analysis. Therefore, the data of the current day, is loaded in the next day, if the vehicle is used. Otherwise it is loaded the next day of use of the vehicle.

Chapter 5

Methodological implementation for leakage detection

This chapter describes in more detail the Oil leakage monitoring methods in hydraulic systems, more precisely a more detailed explanation of the Hilbert-Huang transform and Wavelet transform will be introduced.

5.1 Hilbert Huang transform methodology

The Hilbert-Huang transform is a new developed method for analysing non-stationary data. The key part of such method is the Empirical Mode Decomposition (EMD), this allows that any complicated data-set can be decomposed into a set of finite Intrinsic Mode Functions (IMF), which will admit well-behaved Hilbert Transform. Such method is adaptive which makes it highly efficient.

5.1.1 Empirical Mode Decomposition

A decomposition is a separation of a given signal into different different component, this is usually done in data analysis in order to extract information from the data that it is not possible to obtain considering the data as a whole in the time domain, for such reason the decomposition is a powerful tool to gain insight into some inherent features of the collected data. In general the collected data from the physical model or simulation, is most likely to present one or more of the following problems:

- The total data is too short

- The data are non-stationary, this also applies not only for Fourier analysis, but also for other processes.
- The data represent nonlinear processes

Historically Fourier spectral analysis has provided a general methodology for energy-frequency distributions. The drawback about Fourier analysis is that it is valid under very general conditions. Such conditions are that the system under analysis must be linear and that the data must be strictly periodic or stationary. In general the data obtained is non-stationary, and in terms of linearity, although some systems can be approximated by linear models, in general most of physical systems tend to be nonlinear. Therefore Fourier spectral analysis is of limited use, and it is still used in most of the cases for lack of alternatives.

An alternative for Fourier analysis is the so called Empirical Mode Decomposition method in order to generate a set of Intrinsic Mode Functions [7]. The IMFs are locally non overlapping timescale components having instantaneous frequency and amplitude defined at each point. In addition IMFs are almost orthogonal and form a complete basis set. The effectiveness of the decomposition is evaluated by the index of orthogonality (IO), which shows the independence of each IMF from the others. The IMFs represent the natural mode embedded in the signal. Unlike the classical Fourier analysis which performs global analysis of signals, EMD is a local decomposition method. The procedure to decompose the a signal $x(t)$ into IMFs is the following [8].

First, the local extrema of the signal $x(t)$ are identified. The local maxima are connected together forming the upper envelope $u(t)$ and the local minima are connected forming the lower envelope $l(t)$. This connection is implemented by a cubic spline interpolation. The running mean is defined as:

$$m_1(t) = \frac{l(t) + u(t)}{2} \quad (5.1)$$

Following, $m_1(t)$ is subtracted from the signal $x(t)$, resulting in the first component $h_1(t)$

$$h_1(t) = x_1(t) - m_1(t) \quad (5.2)$$

The component $h_1(t)$ is now examined if it satisfies the conditions to be an IMF, if not, a process called sifting by Huang should be followed until $h_1(t)$ becomes an IMF. In order to be an IMF each component $h_i(t)$, hast satisfy the following conditions:

- The number of extrema and the number of zero crossings must either equal or differ at most by one throughout the whole data set.

- The mean value of the envelope defined by the local maxima and the envelope defined by the local minima is zero at every point.

In the sifting process $h_1(t)$ is treated as new data. The local extrema are identified, the lower and upper envelopes are formed and the associated running mean m_{11} is subtracted from $h_1(t)$ yielding the component $h_{11}(t)$, in the hope that this satisfies the criteria to be an IMF.

$$h_{11}(t) = h_1(t) - m_{11}(t) \quad (5.3)$$

The sifting process is to be repeated many times as required and eventually the component $h_{1K}(t)$ is termed the first IMF of the data series $x(t)$ denoted with C_1 . The first IMF is then subtracted from the the original signal $x(t)$, the difference is called the first residue $r_1(t)$

$$r_1(t) = x(t) - C_1(t) \quad (5.4)$$

The residue $r_1(t)$ is taken as the new signal and the sifting process is applied from the beginning. As a result, the signal $x(t)$ will be decomposed into a finite number of IMFs $C_j(t)$. The sifting process ends when the last residue $r_N(t)$ is a constant or a monotonic function. The signal $x(t)$ is written as the sum

$$x(t) = \sum_{j=1}^N C_j(t) + r_N(t) \quad (5.5)$$

In most practical cases, even extremely complicated time-series can be represented with no more than a few IMFs. Usually, residue $r_N(t)$ possesses no useful information and might be ignored. The IMFs are orthogonal, or almost orthogonal functions, meaning that the signal representation is unique. Neglecting the residue the square of the signal can be written as

$$x^2(t) = \sum_{j=1}^{N+1} C_j^2(t) + 2 \sum_{j=1}^{N+1} \sum_{k=1}^{N+1} C_j(t)C_k(t) \quad (5.6)$$

The cross terms in the right hand of the previous equation should be zero if summed along time. An index of orthogonality (IO) is defined as

$$IO = \sum_{t=0}^T \left\{ \frac{\sum_{j=1}^{N+1} \sum_{k=1}^{N+1} C_j(t)C_k(t)}{x^2(t)} \right\} \quad (5.7)$$

The IO value is used as a criterion for proper decomposition. Typically, values between 0.01 and 0.001 are good enough.

5.1.2 Hilbert-Huang spectrum

The previous described algorithm is the first and most important step in decomposing the non-stationary data. The second and final step is based on the Hilbert transform. The Hilbert transform of a real signal $x(t)$ is defined as [6].

$$y(t) = \frac{1}{\pi} \int_{-\infty}^{+\infty} \frac{x(\tau)}{t - \tau} d\tau \quad (5.8)$$

Then a complex analytic signal is defined as

$$z(t) = x(t) + iy(t) \quad (5.9)$$

The analytic signal can be further expressed as

$$z(t) = A(t)e^{i\theta(t)} \quad (5.10)$$

In the last equation $A(t)$ is the amplitude of the signal envelope and $\theta(t)$ is the instantaneous phase from which the instantaneous signal frequency $f(t)$ is obtained by differentiation.

$$f(t) = \frac{1}{2\pi} \frac{d\theta(t)}{dt} \quad (5.11)$$

Unfortunately, the instantaneous frequency concept is only meaningful for mono-component signals which are symmetric about the local mean. A Solution proposes that the Hilbert Huang transform is applied at all IMFs obtained during the sifting procedure. Indeed, the IMFs are mono-component and locally symmetric functions and therefore the instantaneous frequency is a meaningful feature. The original time-series $x(t)$ is now expressed in a Fourier-like expansion as

$$x(t) = Re \left\{ \sum_{j=1}^N A_j(t) e^{i \int w_j dt} \right\} \quad (5.12)$$

where the subscript j refers to each IMF and $Re\{\cdot\}$ denotes the real part of a complex quantity. The last equation enables us to represent the amplitude and the instantaneous frequency, in a three dimensional plot, in which the amplitude is the height in the time frequency plane. The time-frequency distribution is designated as the Hilbert-Huang spectrum $H(w, t)$. From the Hilbert-Huang spectrum, the marginal spectrum $h(w)$ can be determined as

$$h(w) = \int_0^{T_0} H(w, t) dt \quad (5.13)$$

where T_0 is the total data length. The instantaneous energy $IE(t)$ is defined as

$$IE(t) = \int_{\omega_1}^{\omega_2} H^2(\omega, t) d\omega \quad (5.14)$$

The marginal spectrum $h(\omega)$ measures the contribution of each frequency component, while the instantaneous energy $IE(t)$ provides information about the time variation energy. MATLAB is capable of performing the HHT by already taking into account all the previous mentioned steps, thus this will be used in this project.

5.2 Wavelet transform methodology

The wavelet transform is a signal processing tool that decomposes a non-stationary signal into levels (also known scales) with different time and frequency resolutions [5]. As opposed to Fourier analysis that breaks up a signal into sine waves of different frequencies, wavelet analysis breaks up a signal into shifted and scaled versions of the original (mother) wavelet. For non-stationary signals, the Fourier analysis is not effective since it transforms the signal into the frequency domain and the time information is lost. This deficiency of the Fourier analysis can be removed to some extent by analyzing a small section of the signal at a time, this is a technique called windowing. This type of analysis, known as the short-time Fourier transform (STFT), however has the drawback in that the size of the time window is the same for all frequencies and is computationally expensive. Wavelet analysis, on the other hand, allows a windowing technique with variable-size regions. Long time intervals are used to obtain low-frequency information about the signal, shorter time regions are chosen when high-frequency information is needed. Furthermore, past studies have indicated that, as compared to STFT, WT yields results from which faults are clear to distinguish and easy to interpret. WT can be continuous (CWT) or discrete (DWT). The CWT is defined as the sum over all time of the signal multiplied by the scaled and shifted versions of the wavelet function ψ .

$$CWT(a, b) = \frac{1}{\sqrt{a}} \int_{-\infty}^{+\infty} x(t) \psi \left(\frac{t-b}{a} \right) dt \quad (5.15)$$

where $\psi(t)$ is the mother wavelet and can be a complex conjugate. $a, b \in R$ (R is a real continuous number system) denotes the "scaling" and "shifting" parameters, respectively. For most practical applications, the wavelet coefficients are discretized by a factor of $2^m n$ for shift and by a factor of 2^m for scaling. The previous equation can then be defined as

$$DWT(m, n) = 2^{-m/2} \int_{-\infty}^{+\infty} x(t) \psi \left(2^{-m} t - n \right) dt \quad (5.16)$$

Where m and n are integers. There exists a well-known algorithm, known as "multiresolution signal decomposition technique", for fast implementation of DWT. It is computed by a successive low and high pass filtering of the discrete signal $x[n]$. The wavelet decomposition process starts by applying the low and high pass

analysis filters on the original signal, resulting a_1n and $d_1[n]$ have $n/2$ points each. Thus, the decomposition process can be continued, with successive approximations being decomposed in turn, so that the original signal is broken down into many lower resolution components.

5.3 Predictive Maintenance Algorithm development

The idea behind algorithm development is to use data of healthy and faulty conditions, such data follows a pre-processing step in order to distinguish the condition indicators which can differentiate healthy from faulty operation, the following project arrives until this point

In some occasions it is possible to train an artificial intelligence algorithms that will be capable to distinguish between these fault and healthy states of the machine, however bibliographic review [2] explains that machine learning training for fluid systems has not yet had sufficient experimentation, therefore more research needs to be done in such aspect. For such reason this thesis document limits itself on signal processing techniques for failure identification.



Figure 5.1: Algorithm development process

5.3.1 Data Acquisition

The first step for the process is to collect sensor data, such data should represent two states of the machines, that is, healthy and faulty operation. In this sense it will be possible in the future to develop algorithms capable of identifying between these two conditions. It is better if such data can be collected under various types of situations, like different temperatures, different operating conditions in order to have a richer data-set. In some cases it is not possible to rely on healthy and faulty data of the system of interest, for such case it is possible to use a mathematical model of the system that may simulate healthy and faulty operation. Currently in the project described in this document, the data acquisition system has already been constructed and installed in the targeted hydraulic system. However, since the system is new, it is only acquiring healthy data, in order to collect faulty data as well there has to exist a time lapse, which is not possible to determine with a

good degree of certainty. For such case a mathematical model-based approach was be used.

5.3.2 Data pre-processing

Once the data has been acquired it is necessary to do pre-process stage in order to be able to extract some useful information from it. Such pre-processing actions are for instance noise extraction, outlier, and missing value removal. In many cases additional pre-processing can be done like conversion to time domain to frequency domain.

5.3.3 Condition Indicators

One the data has been pre-processed, now it is possible to extract information from the current processed data in order to develop a capable algorithm able to identify failures. Such indicators are variations of the system behavior when operating in healthy fan faulty conditions. For example while working in frequency domain, when the system operates in normal conditions (without fault), the dynamics operate under a certain frequency domain, on the other hand when the system operates in faulty conditions, since we have an imminent failure, this will force the system to change its dynamic behavior, thus also changing the frequency domain slightly. Such difference, in many cases small ones will allow us to determine the states between healthy and faulty operation.

For this project, the condition indicators in wavelet transform were the detail and approximate coefficients, on the other hand using HHT, the instantaneous amplitude was used as condition indicator

Chapter 6

System modelling for data acquisition

In previous chapters it was mentioned that in order to detect possible failures in any system by means of the proposed methodology, it is necessary to have data of the current system working in optimal conditions and in failure conditions. For this purpose by the time this project has been developed, the data acquisition system was already mounted and ready to collect data, however the data acquisition period was quite short, giving us data only of the system working in normal healthy conditions, this means with no apparent failure. In order to obtain data of the system in failure conditions, it was necessary to collect data for a much longer period of time.

Given the data constraints, a way to overcome such difficulties was to implement a mathematical model of the hydraulic system with the failures included in order to collect the unavailable failure data that the real system at that moment was unable to provide, the model was implemented in Simulink and is explained in detail in this chapter.

Since the most critical case was leakage mostly in the cylinders, due to the working pressure conditions in the compaction process, however it is also important to know that leakage also occurs in other systems components such as the pump, the control valves and the pressure relief valves. For this project, as previously stated, only the analysis of the cylinder leakage was performed using the frequency decomposition methods explained in Chapter 5. The dynamic development of the equations are related used from different bibliographic sources [9], [10], [5].

Since each component failure can be treated independently, each failure cause can be analyzed independently from the others. The reader is free to review the literature of pump failure detection, or any other component of the system that is not described here.

6.1 Hydraulic cylinder leakage Modelling

In this section a sufficiently approximate model of the real system was derived. It was necessary to understand that in the cylinder-shovel rotation system, there are a pair of actuators, however each cylinder presents the same displacement from the other, therefore only one cylinder can be modelled in order to capture the dynamic behavior from both. Same idea applies to the large cylinder that perform the compaction operation.

For the system modelling it will be assumed that the pressure supplied by the pump is a constant one. The main focus will be centered in the hydraulic cylinder actuated by the control valve. Given that the control valve plays a very important role in the cylinder dynamics, a description of the valve functioning will be also done.

6.1.1 Control Valve analysis

The control valve used for this hydraulic systems is a 4 way three position spool valve, the most widely used control valves are commonly the so called sliding valves employing a spool type construction. Moreover the vast majority of four-wave valves are manufactured with a critical center because of the emphasis on the linear flow gain. A critical center or zero lapped valve has a land width identical to the port width and is a condition approached by practical machining. The valve which composes the system which was analyzed enters into the category of a sliding and critical center valve, the.

Consider the valve presented in Figure 6.1. The arrows at the ports indicate the assumed directions of flows and the area at the ports. We choose the zero position $x_v = 0$ of the spool at the neutral position of the valve.

At this point we are interested in steady-state characteristics, the compressibility of the flows are zero and the continuity equations for the two valve chambers are:

$$Q_L = Q_1 - Q_4 \tag{6.1}$$

$$Q_L = Q_3 - Q_2 \tag{6.2}$$

A dynamic analysis would require an inclusion of the compressibility flows which depends on the valve chamber volumes, this is analyzed later into this chapter.

$$P_L = P_1 - P_2 \tag{6.3}$$

Where Q_L is the flow through the load P_L is the pressure drop across the load.

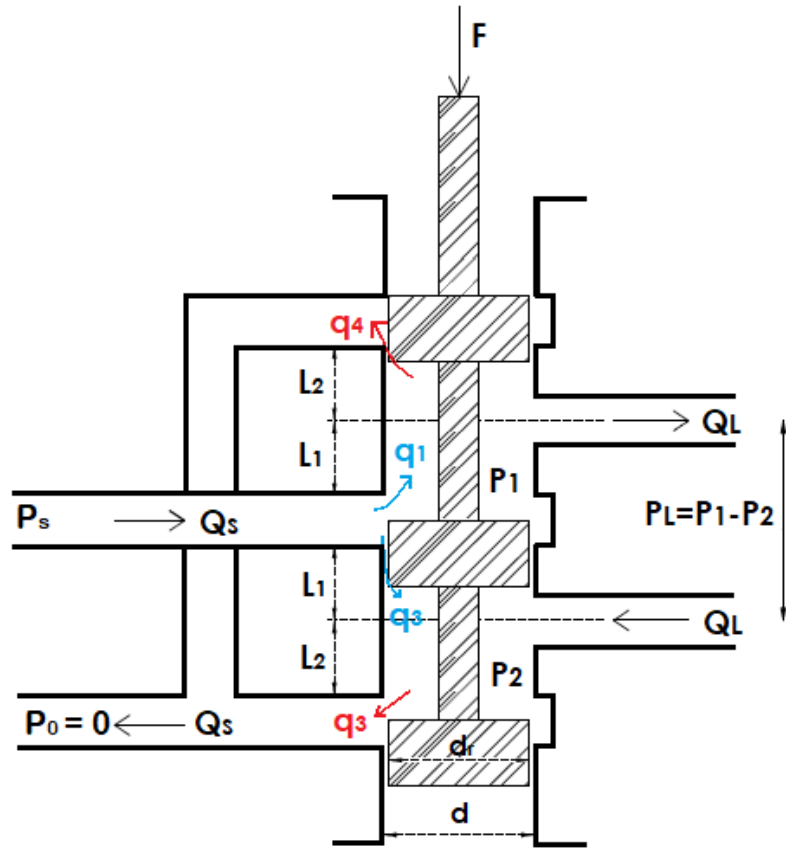


Figure 6.1: Four-way spool valve

From Bernoulli equation we obtain the flows through the valving orifices.

$$Q_1 = C_d A_1 \sqrt{\frac{2}{\rho} (P_s - P_1)} \quad (6.4)$$

$$Q_2 = C_d A_2 \sqrt{\frac{2}{\rho} (P_s - P_2)} \quad (6.5)$$

$$Q_3 = C_d A_3 \sqrt{\frac{2}{\rho} (P_2)} \quad (6.6)$$

$$Q_4 = C_d A_4 \sqrt{\frac{2}{\rho} (P_1)} \quad (6.7)$$

Where C_d is the discharge coefficient which normally takes values between 0.6 and 1. A_i corresponds to the area of each orifice of the valve, which is dependent of x_v , ρ is the fluid density. In the vast majority of cases the valving orifices are matched and symmetrical, this is because the displacement x_v varies equally for all the spool components. Thus, we can derive the following expressions.

$$A_1 = A_3 \quad (6.8)$$

$$A_2 = A_4 \quad (6.9)$$

moreover, symmetrical orifices require that

$$A_1(x_v) = A_2(-x_v) \quad (6.10)$$

$$A_3(x_v) = A_4(-x_v) \quad (6.11)$$

For this reason, the neutral position of the spool for all four orifice areas are equal.

$$A_1(0) = A_2(0) = A_3(0) = A_4(0) = A_0 \quad (6.12)$$

If the orifices areas are linear with valve stroke, as it is usually the case, a parameter needs to be defined in order to compute the rate of change of orifice area with stroke, such parameter is the area gradient of the valve w which is in m^2/m , this will be better clarified later. If the orifices are both matched and symmetrical, the flows in diagonally opposite orifices of the valve have the following relations.

$$Q_1 = Q_3 \quad (6.13)$$

$$Q_2 = Q_4 \quad (6.14)$$

Substituting the given expression with the flow equations for each orifice, we obtain the following relations

$$C_d A_1 \sqrt{\frac{2}{\rho}(P_s - P_1)} = C_d A_3 \sqrt{\frac{2}{\rho}(P_2)} \quad (6.15)$$

Since $A_1 = A_3$, this gives the result.

$$P_s = P_1 + P_2 \quad (6.16)$$

It is possible to use equation 6.16 and replace it on equation 6.3 to obtain P_1 and P_2 , in terms of P_s and P_L , which are equations 6.17 and 6.18

$$P_1 = \frac{P_s + P_L}{2} \quad (6.17)$$

$$P_2 = \frac{P_s - P_L}{2} \quad (6.18)$$

Once this analysis has been done, it can be used for treating in the critical center valve cases. Critical center valves can have ideal or practical geometry. Ideal geometry implies that the orifice edges are perfectly square with no rounding and that there is no radial clearance between the spool and the sleeve. Although these geometrical perfections are not possible in practice, however it is possible to construct a valve with a relatively linear flow gain near null position. Such critical center valve with practical geometry, that is, with radial clearance, is in many respects an optimum valve because leakage flows are minimum.

Now using the previously detailed equations, it is possible to derive more generic equations for an ideal valve with matched and symmetrical orifices.

The leakage flows (Q_2 and Q_4 when x_v is negative and Q_1 and Q_3 when x_v is positive), for such valves are assumed to be zero because the geometry is assumed to be ideal. Therefore Using equations 6.17 and 6.4 into 6.1

We obtain for for $x_v > 0$

$$Q_L = C_d A_1 \sqrt{\frac{2}{\rho} (P_s - P_L)} \quad (6.19)$$

For $x_v < 0$, equation 6.2 can be used in a similar manner with a negative valve displacement, we have the following expression.

$$Q_1 = -C_d A_2 \sqrt{\frac{2}{\rho} (P_s + P_L)} \quad (6.20)$$

Because the valve is assumed to be symmetrical the previous two equations can be combined into a single one.

$$Q_1 = -C_d w x_v \sqrt{\frac{1}{\rho} (P_s + \text{sgn}(x_v) P_L)} \quad (6.21)$$

where w was introduced before, is the area gradient of the valve w which is in m^2/m . Replacing the value of $P_L = 2P_1 - P_s$ using P_1 and $P_L = P_s - 2P_2$, we have the final two expression for orifice flow.

Inlet flow

$$Q_L = K_v w x_v \sqrt{\frac{P_s}{2} + \text{sgn}\left(\frac{P_s}{2} - P_1\right)} \quad (6.22)$$

Outlet flow

$$Q_L = K_v w x_v \sqrt{\frac{P_s}{2} + \text{sgn}(P_2 - \frac{P_s}{2})} \quad (6.23)$$

This two expressions will be of great help in the dynamic modelling of the cylinder with the valve.

6.1.2 Hydraulic cylinder dynamic modelling

The combination of servovalves and pistons is quite common in hydraulic power elements. For developing the model we use the law of conservation of mass, which is also called the continuity equation, the form given is adequate for the analysis of fluid components.

$$\sum W_{in} - \sum W_{out} = g \frac{dm}{dt} = g \frac{d(\rho V_0)}{dt} \quad (6.24)$$

Where W are the weight flow rates into and from the volume, V_0 is the accumulated or stored mass of fluid inside, m is the mass of the fluid which has its equivalent expression as a function of Volume V_0 and the fluid density ρ . Thus the continuity equation can be written in the following way.

$$\sum W_{in} - \sum W_{out} = g \frac{d(\rho V_0)}{dt} = g\rho \frac{dV_0}{dt} + gV \frac{d\rho}{dt} \quad (6.25)$$

It is also possible to write the weight flow rate in the following manner $W = g\rho Q$ and therefore combining the previous equation with such expression. Thus we obtain a more useful expression for practical purposes.

$$\sum Q_{in} - \sum Q_{out} = \frac{dV_0}{dt} + \frac{V_0}{\beta} \frac{dP}{dt} \quad (6.26)$$

Where β is the fluid bulk modulus. The first term of the right hand side corresponds to the the flow consumed by the expansion of the control volume, this term is zero if the volume is fixed. The second term is the compressibility flow, it describes the flow resulting from pressure changes.

Applying equation 6.26 to our system, which is presented in In Figure 6.2, we can derive the following two equations.

$$Q_1 - k_{il}(P_1 - P_2) = \frac{dV_1}{dt} + \frac{V_1}{\beta_e} \frac{dP_1}{dt} \quad (6.27)$$

$$k_{il}(P_1 - P_2) - k_{el}P_2 - Q_2 = \frac{dV_2}{dt} + \frac{V_2}{\beta_e} \frac{dP_2}{dt} \quad (6.28)$$

where each equation correspond to each of the hydraulic cylinder chambers. V_1 :
Volume of the forward chamber m^3

V_2 : Volume of the forward chamber m^3

k_{il} : Internal leakage coefficient of the piston $\frac{m^3}{\sqrt{Pas}}$

k_{el} : External leakage coefficient of the piston $\frac{m^3}{\sqrt{Pas}}$

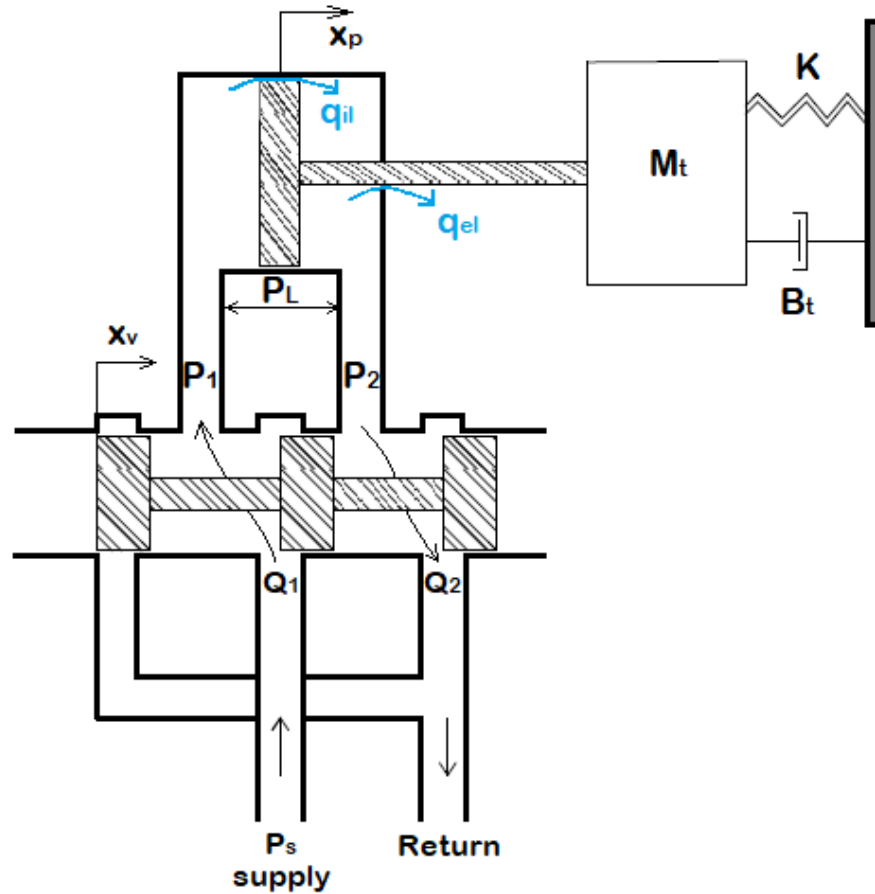


Figure 6.2: Failure cylinder-valve system

The volumes of the piston chambers may be written in the following way:

$$V_1 = V_{01} + A_{1p}x_p \quad (6.29)$$

$$V_2 = V_{02} - A_{2p}x_p \quad (6.30)$$

where

A_p : Area of the piston, m^2

x_p : displacement of piston, m

V_{01} : Initial volume of the forward chamber, m^3

V_{02} : Initial volume of the return chamber, m^3

Replacing 6.29 and 6.30 into equations 6.27 and 6.28, we obtain the following expressions

$$Q_1 - k_{il}(P_1 - P_2) = \frac{d(V_{01} + A_{1p}x_p)}{dt} + \frac{V_{01} + A_{1p}x_p}{\beta_e} \frac{dP_1}{dt} \quad (6.31)$$

$$k_{il}(P_1 - P_2) - k_{el}P_2 - Q_2 = \frac{d(V_{02} - A_{2p}x_p)}{dt} + \frac{V_{02} - A_{2p}x_p}{\beta_e} \frac{dP_2}{dt} \quad (6.32)$$

Moreover using equations 6.31 and 6.32, the last that describes the flow through and orifice we obtain the following equations.

$$\dot{P}_1 = \frac{\beta_e}{V_{01} + A_{p1}x_p} (Q_1 - k_{il}(P_1 - P_2) - A_{p1}v_p) \quad (6.33)$$

$$\dot{P}_2 = \frac{\beta_e}{V_{02} - A_{p2}x_p} (-Q_2 + k_{il}(P_1 - P_2) + A_{p2}v_p) \quad (6.34)$$

Finally replacing for Q_L , we obtain a couple of equations that describe the behavior of flow inside the hydraulic piston.

The final equation that describes the dynamic behavior arises from Newton's second law.

$$F = ma$$

$$AP_1 - AP_2 - d\dot{x}_p = m\ddot{x}_p \quad (6.35)$$

$$\dot{P}_1 = \frac{\beta_e}{V_{01} + A_{p1}x_p} \left(K_v w x_v \sqrt{\frac{P_s}{2} + \text{sgn}\left(\frac{P_s}{2} - P_1\right)} - k_{il}(P_1 - P_2) - A_{p1}v_p \right) \quad (6.36)$$

$$\dot{P}_2 = \frac{\beta_e}{V_{02} - A_{p2}x_p} \left(-K_v w x_v \sqrt{\frac{P_s}{2} + \text{sgn}\left(P_2 - \frac{P_s}{2}\right)} + k_{il}(P_1 - P_2) - k_{el}P_2 + A_{p2}v_p \right) \quad (6.37)$$

The system states are the actuator position x_p , the actuator velocity v_p , and the line pressures P_1 , P_2 . The parameters are the mass load m , the effective viscous

damping of the actuator d , the parameters A refers to the annulus area of the piston. V is the the volume of the fluid contained on either side of the actuator when it is centered. Parameter K_v is the the valve flow gain, and w is the area gradient. P_s is the supply pressure, which is considered constant.

$$q_{el1} = k_{el}P_1 \quad (6.38)$$

$$q_{el2} = k_{el}P_2 \quad (6.39)$$

$$q_{il} = k_{il}(P_1 - P_2) \quad (6.40)$$

k_{el} and k_{il} are leakage coefficients whose values depend on the severity of leakage fault. It is important to see that q_{el1} , q_{el2} and q_{il} are zero for an actuator working in normal operating conditions.

Final fault-dynamic equations of the hydraulic cylinder

The system is a nonlinear dynamic system, the equations describing the actuator dynamics are the following:

$$\dot{x}_p = v_p \quad (6.41)$$

$$\dot{v}_p = \frac{1}{m}(AP_1 - AP_2 - dv_p) \quad (6.42)$$

$$\dot{P}_1 = \frac{\beta}{V_{01} + Ax_{p1}} \left(K_v wx_v \sqrt{\frac{P_s}{2} + \text{sgn}(x_v) \left(\frac{P_s}{2} - P_1 \right)} - q_{il} - A_{p1}v_p \right) \quad (6.43)$$

$$\dot{P}_2 = \frac{\beta}{V_{02} - Ax_{p2}} \left(-K_v wx_v \sqrt{\frac{P_s}{2} + \text{sgn}(x_v) \left(P_2 - \frac{P_s}{2} \right)} + q_{il} - q_{el2} + A_{p2}v_p \right) \quad (6.44)$$

6.2 Matlab System Modelling

For the simulation of the dynamic system it was used the Simscape tool of matlab. Simscape is a Matlab tool that enables the user to model and simulate multidomain physical systems, they can be rapidly created within the Simulink environment. Simscape also helpsto develop control systems and test system-level performance,

thus it has a quite reliable approximation to real performance of systems. It is possible to custom component models using the MATLAB based Simscape language, which enables text-based authoring of physical modeling components, domains, and libraries.

For our data generation a single model will be created, the leakages will be simulated using valves which can change the orifice size in order to let simulate a leakage outside of the system for external leakages or inside of the system between the cylinder chambers in order to simulate internal leakage of the fluid.

The main characteristics of the model are the following:

- Internal leakage among the chambers of the cylinder is modelled with a variable orifice block or a needle valve.
- External leakage modelling uses the same principle as the previous point, however the leaked fluid flows from the system to the reservoir.
- The pump provides a constant pressure to the system, which is modelled as a constant pressure block to the system.
- The trash to be compacted is modelled as a mass-spring-damper system.

As it is possible to visualize in Figure 6.3 we can see the general representation of the system with four inputs and two outputs. The first two inputs labeled as "valve opening" correspond to the needle valve opening in millimeters that simulate the system leakage internal and external.

The outputs that will be analyzed are the piston position and the pressure, overall the pressure is of main focus in order to analyze it's variations due to leakages.

Figure 6.4 represents each subsystem necessary to model the overall hydraulic system, where it is possible to see the valve command subsystem which gives the the necessary signals in order to move the 3 position control valve to move the cylinder forward, backwards or keep it on neutral position. the compaction subsystem models the mass-damper-spring behavior which simulates the process of garbage compaction. The supply pressure system which provides a constant pressure of 120 Mpa to the system which works in normal operation conditions. Finally the valve-cylinder subsystem, which models the 3 way position control valve with the cylinder linear displacement.

Figure 6.5 shows in more detail the cylinder-valve subsystem, it is possible to see that in order to simulate the leakage behavior, two needle valves are introduced, one for simulate internal leakage modelling and the other for simulate the external leakage modelling. Both can variate the distance opening, therefore the opening area of the valve can also variate in order to simulate from small to higher leakages. From such possibilities, the next chapter will deal in more detail about the results

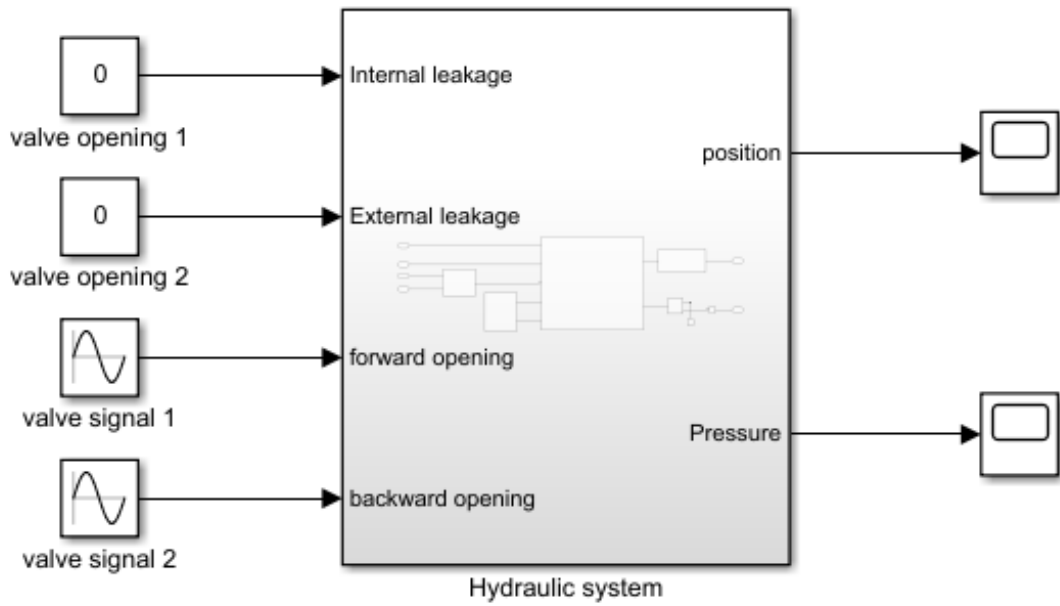


Figure 6.3: Hydraulic system general modelling

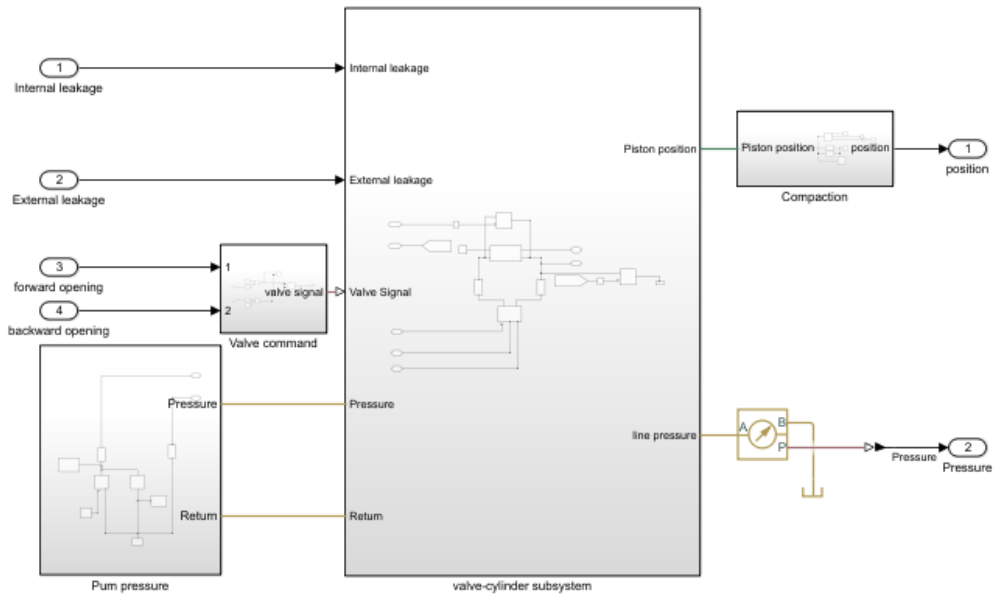


Figure 6.4: Overview of subsystems

of such simulations and will show the practical use of leakage detection methods

that were previously introduced.

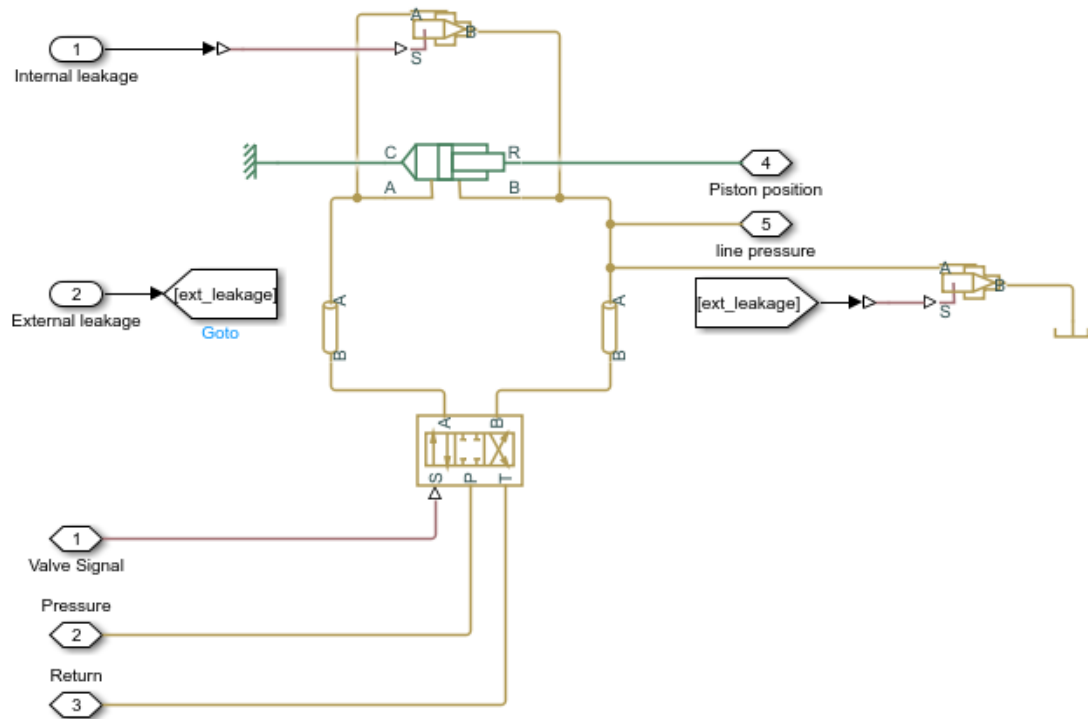


Figure 6.5: Valve-cylinder modelling

Chapter 7

System simulation, fluid leakage detection and final results

The simulation of the system comprises two main areas. First one the simulation related to external leakage and in second place the simulation of internal leakage of the hydraulic cylinder.

7.1 External leakage

External leakage causes a static pressure drop in the system, since a part of fluid is lost from the hydraulic circuit. As we can see in Figure 7.1 it is possible to understand this pressure drop on the system, however the dynamic behavior is quite similar to healthy operating conditions, with the addition that the fault response has a drift in comparison with normal operating conditions.

Wavelet approach for external leakage detection

In order to detect such pressure drift, this will appear in coarser scales represented by approximation coefficients of wavelet decomposition. For such reason approximation coefficients of pressure signals are a good approach to detect external leakage.

The idea is the following since the approximation coefficients are the result of a low filtered in the wavelet decomposition it is possible to analyze only the drift on the signal between healthy and faulty operating conditions. It will be used the scale a_4 of approximation coefficients for external leakage detection. RMS values will be computed for each approximation coefficient in order to detect failures.

Since healthy operating conditions have the highest steady state pressure value, because it does not have a drift, it had the highest RMS value of the estimated approximation coefficient. On the other hand the more leakage it is presented the higher was the drift in the system response and therefore the lower the RMS value obtained by computing the approximation coefficient.

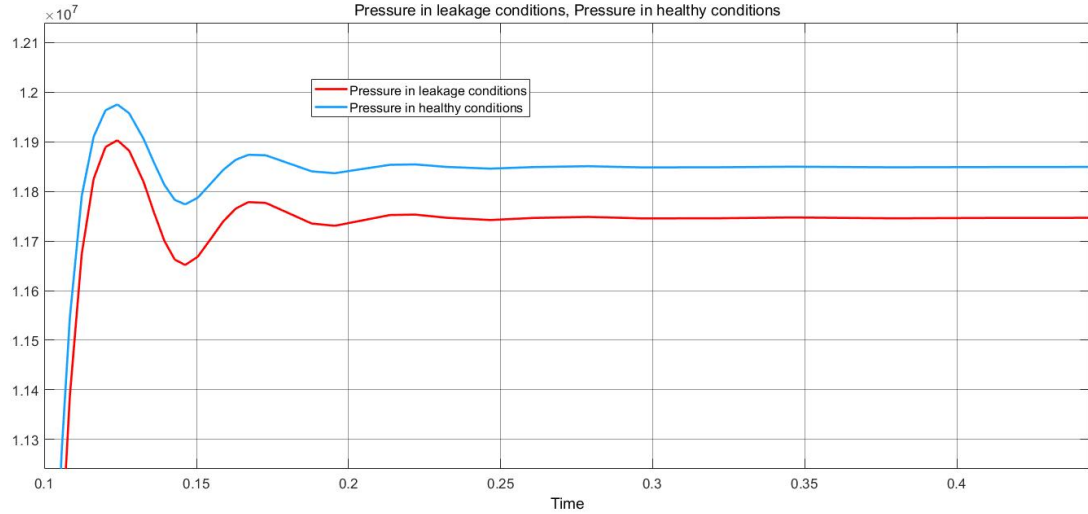


Figure 7.1: Pressure output with internal leakage

7.2 External Leakage simulation

For the leakage detection in the system operating in normal conditions, a Matlab script was written where the simulation of the system was performed in several occasions. where the valves opening variate from zero and gradually opened to simulate from very small to higher amounts of fluid leakage in the system. This allowed to detect the minimum possible leakage rate. The simulations followed the order in which the valve opening value started at zero and gradually increased among each simulation, going from a small leakage fault to a high leakage fault. The description is specified below:

- First simulation
 - Valve closed.
 - Leakage: no leakage.
- Second simulation:

- Valve opening: 5 μm .
- Leakage: 0.24 L/min (small leakage).
- Third simulation:
 - Valve opening: 25 μm .
 - Leakage: 1.20 L/min (medium leakage).
- Fourth simulation:
 - Valve opening: 45 μm .
 - Leakage: 2.14 L/min (Large leakage).

First simulation

As it is possible to visualize in Figure 7.2 the different wavelet approximation coefficients were estimated, it is known [5] that scale a_4 is used for external leakage detection having little computational burden as well as good sensitivity for fault type. Since the valve is closed no fluid is lost.

Second simulation

For the second simulation the valve opening was set to $5\mu\text{m}$ which leads to an average fluid leakage of 0.24 L/min. The wavelet decomposition is shown in Figure 7.3. The leakage simulation is presented in Figure 7.4, from which the average leakage value is approximately $4 \times 10^{-6} (m^3/s)$. In a similar way as before approximation coefficient a_4 was used for leakage detection purposes.

Third simulation

For the third simulation the valve opening was set to $25\mu\text{m}$, giving an average leakage in the cylinder of 1.2 L/min. The wavelet decomposition approximation coefficients are shown in Figure 7.5. The leakage simulation is presented in Figure 7.6, from which the average leakage value is approximately $2 \times 10^{-5} (m^3/s)$. Later it will be presented the RMS value computation of approximation coefficient a_4 in order to detect leakage failures.

Fourth simulation

In the Fourth simulation the valve opening was set to $45\mu\text{m}$, giving an average leakage in the cylinder of 2.14 L/min which comes from the average leakage value computed by Simscape which is $3.56 \times 10^{-5} (m^3/s)$. In a same manner as before approximation coefficients are obtained from the wavelet decomposition, then the RMS value of the a_4 coefficient is estimated.

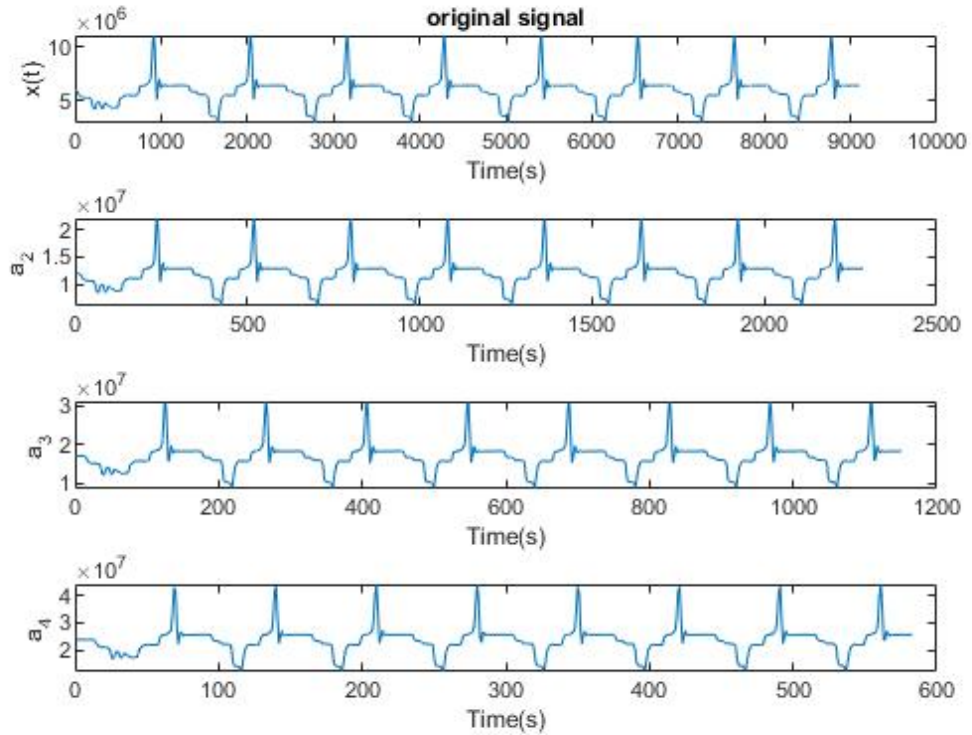


Figure 7.2: Wavelet decomposition, hydraulic cylinder with no leakage

7.2.1 External leakage results

The four simulations shown previously were performed setting the cylinder at 6 Mega Pascals as initial conditions for each chamber from which the following table results:

In a similar way, five experiments were performed each one having the four simulations with the same variability of valve openings leading to the same leakage values. This was done in order to obtain several experiments with different initial conditions in order to set a threshold value at which the signal decomposition technique was able to detect leakages. Figure 7.7 shows the results of each simulation. If we take for instance the first experiment which contained the four simulations, it is possible to visualize how the RMS value of the approximation coefficient a_4 diminishes each time the leakage fault increases, which is in accordance to what was previously discussed. The main cause is the drift which is originated by the static pressure loss of the system, in a similar way the other experiments can be verified.

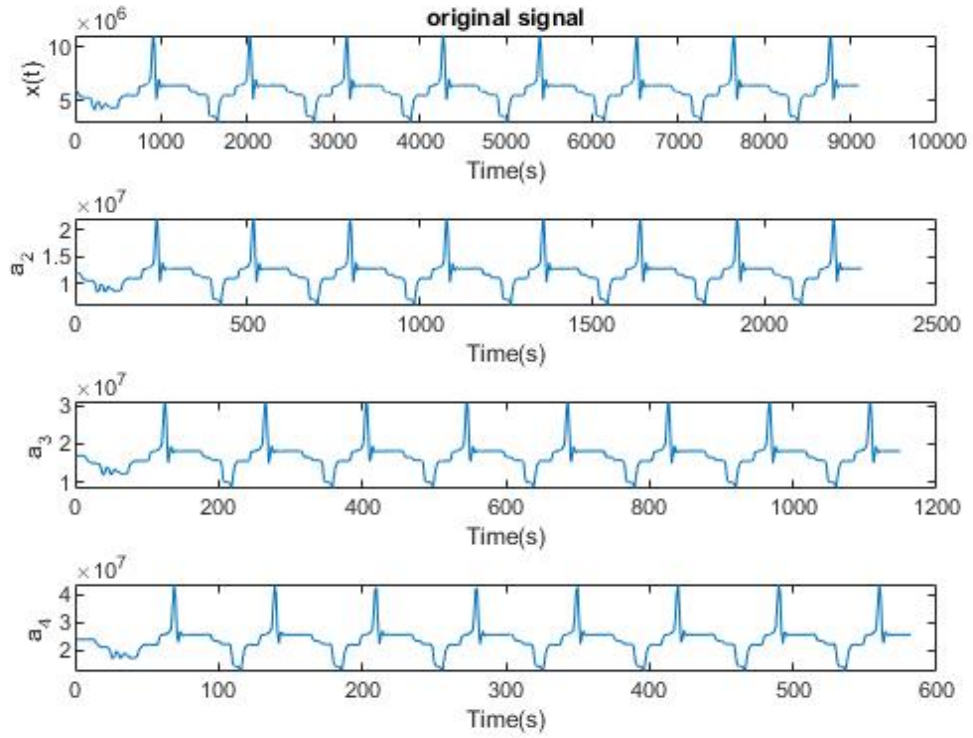


Figure 7.3: Approximate coefficients of wavelet decomposition, hydraulic cylinder with small external leakage

Valve opening $\mu\text{ m}$	Leakage level	Mean leakage L/min	RMS scaled	% of change
0	No leak	0	1	0
0.005	small leak	0.24	0.982	1.773
0.025	medium leak	1.2	0.972	2.802
0.045	large leak	2.136	0.961	3.851

Table 7.1: First experiment results with WT methodology for external leakage detection

Finally it is possible to visualize that in this case it is somehow difficult for the signal processing to distinguish between a closed valve and a small leakage failure, since their values overlap in the graphic. On the other hand it is clear that this

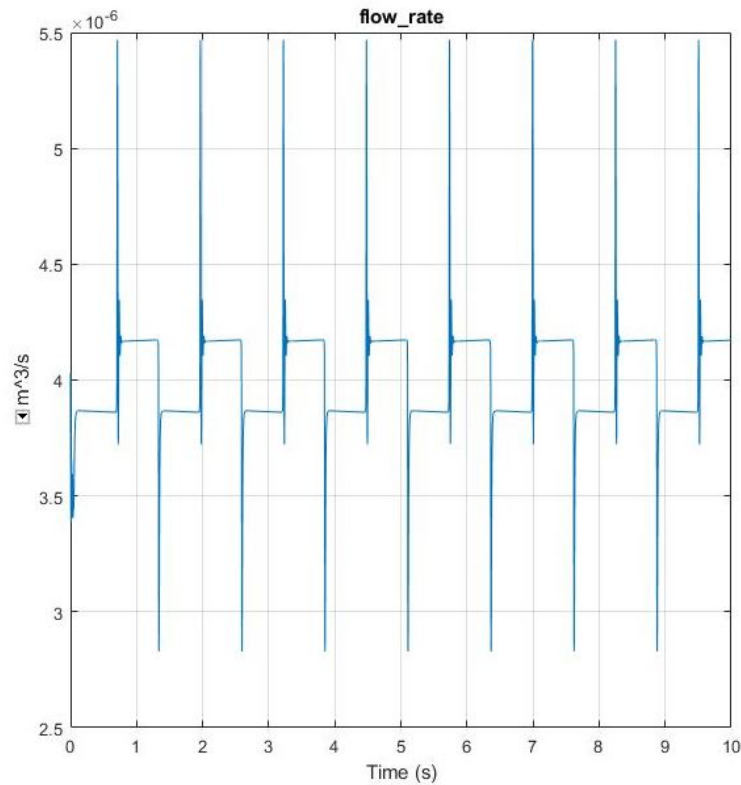


Figure 7.4: Leakage measurement of the valve opened at 5 micrometers

is not the case for medium leakage faults. For such reason a threshold line was drawn indicating such separation. In this manner it is possible to infer that the methodology proposed in this case is able to detect medium leakage faults.

It is also very important to mention that a leakage fault is very difficult to model since according to bibliography [4], it contains a lot of uncertainties, this can be to some extent due to the geometry of the fault orifice which has an irregular shape and tends to vary in diameter along the piston seals. For this reason a good model of an hydraulic actuator which takes into account such failures is still a challenge nowadays. Simscape, is able to perform a reasonable model at a certain extent. However, real experiments which operate with real data of hydraulic cylinder failures are able to give a better results in the percentage of change of the RMS values, the values that separate the different leakage levels discussed in this document tend to be larger and therefore a better separation among healthy and faulty conditions can be done.

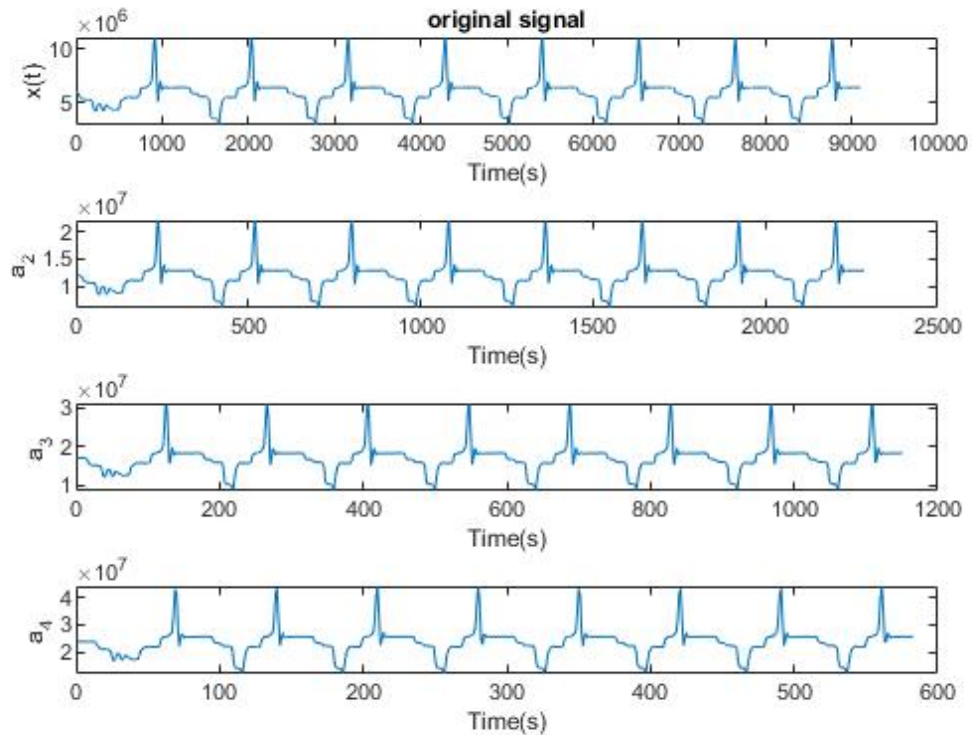


Figure 7.5: Approximate coefficients of wavelet decomposition, hydraulic cylinder with medium external leakage.

7.3 Internal leakage

For internal leakage purposes internal leakage models proposed by [4] and [10] were used since the Simscape modelling was not able to represent in a clear manner the damping effect with the needle valve which simulated internal leakage on the system.

Internal leakage failure alters the transient responses in the line pressure. This is caused because when internal leakage increases, it tends to increase also the cylinder damping. As a result the higher is the internal leakage flow between the cylinder chambers the higher will be the damping coefficient. According to bibliography[4], it is experimentally verified that in normal operating conditions the amplitude and energy of the system response are higher than those obtained by systems with internal leakage. Since we have a reduction in energy and amplitude of the system. This was done in the modelled system for this thesis project on Figure 7.8

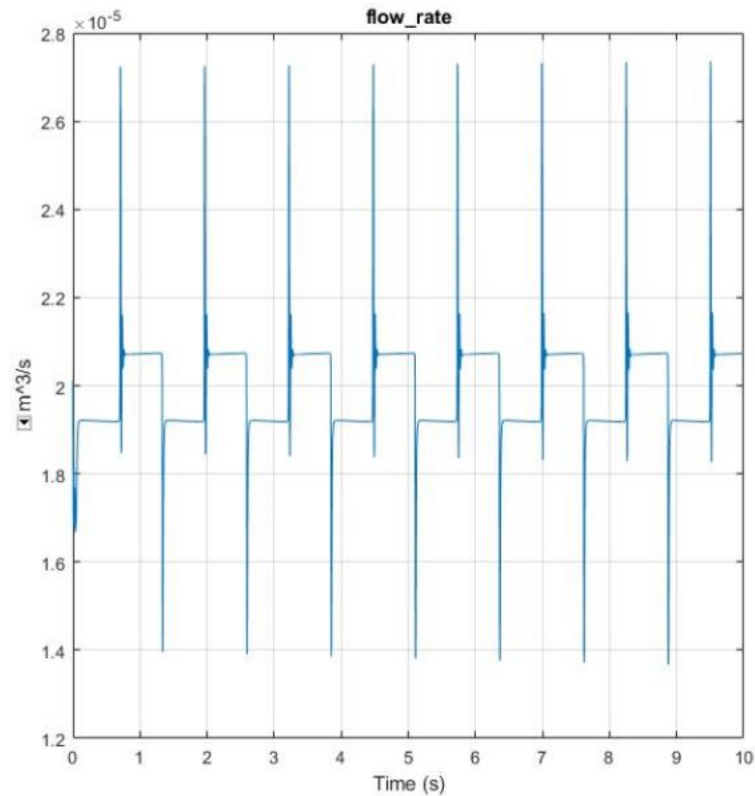


Figure 7.6: Leakage measurement of the valve opened at 25 micrometers

Wavelet approach for internal leakage detection

The friction of the piston seal has a damping behavior, however in faulty conditions, the orifice in the piston seals acts also like a damper which tends to increase the damping behavior if the orifice size also increases.

The used approach for internal leakage detection is based on the analysis of detail wavelet coefficients which represent in a better way the transient response of a cylinder chamber. The detail coefficients are related to high frequency information of the pressure signal, when the system operates at normal conditions the detail coefficients are able to capture all high frequencies of the system. On the other hand if we have internal leakage, as previously mentioned, the energy and amplitude of the system are reduced by the increment of a damping coefficient, therefore it is expected to see a reduction in higher frequencies when the leakage fault increases, this is represented by the detail coefficient.

In order to analyze each output response the root mean squared value is taken from the detail coefficients from normal and faulty simulations responses. The

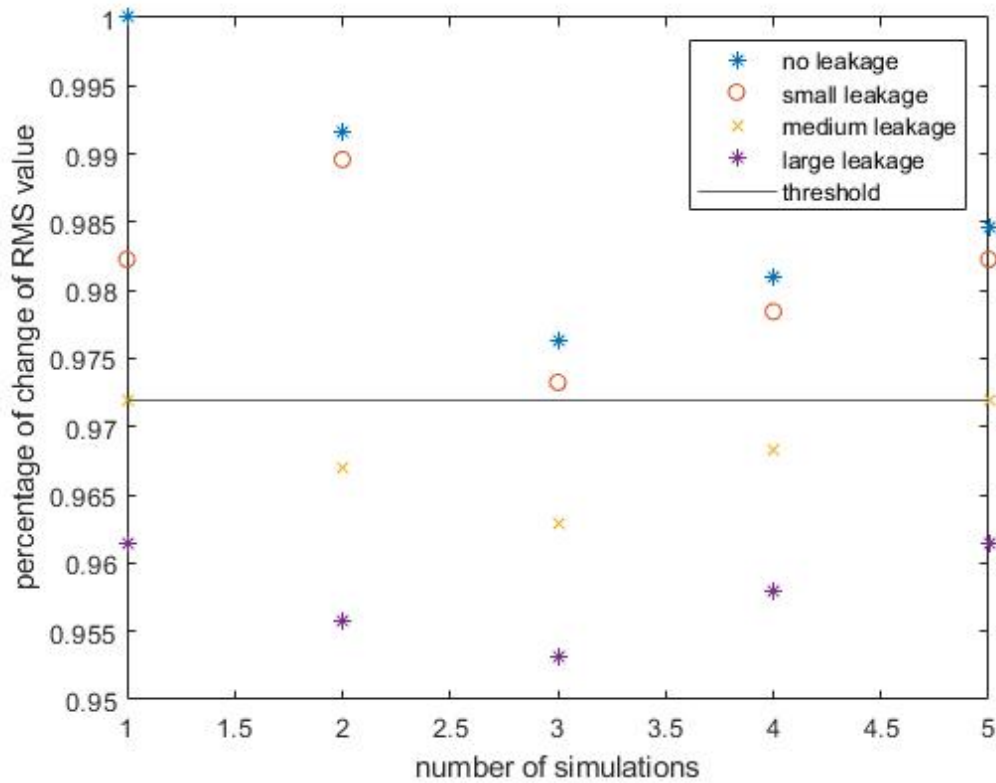


Figure 7.7: External leakage detection results

smaller RMS value of a given coefficient, the more severe is the internal leakage.

The approximate coefficients remain unchanged in this case, thus are not used for internal leakage detection, approximate coefficients contain low frequency information of the signal.

Hilbert-Huang approach for internal leakage detection

The leakage detection procedure is very similar as in the wavelet case, however in this case the RMS value of the instantaneous amplitude was calculated in order to detect between healthy and faulty conditions. As mentioned before internal leakage reduces the energy and amplitude of the system response. Thus a healthy system operating in normal conditions should have a higher instantaneous amplitude RMS VALUE than a system with internal leakage, which due to the damping effect will have a lower instantaneous amplitude.

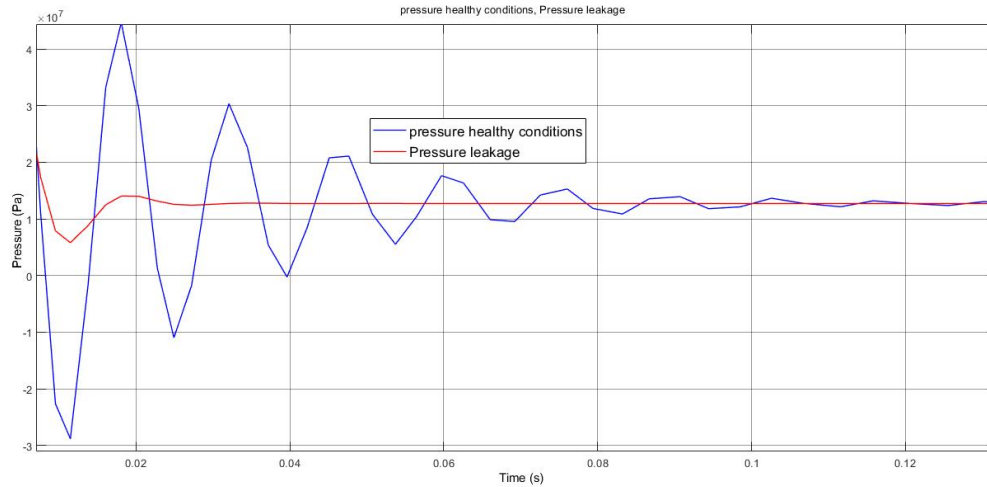


Figure 7.8: healthy and fault conditions step response

7.3.1 Internal leakage Wavelet decomposition results

In this section the results of the simulations are presented. For either simulations, the Wavelet decomposition analysis and the Hilbert Huang transform the same valve openings were used, leading to the same leakage amounts in each case.

- First simulation
 - Valve closed.
 - Leakage: no leakage.
- Second simulation:
 - Valve opening: 5 μm .
 - Leakage: 0.36 L/min (small leakage).
- Third simulation:
 - Valve opening: 20 μm .
 - Leakage: 1.08 L/min (medium leakage).
- Fourth simulation:
 - Valve opening: 40 μm .
 - Leakage: 1.65 L/min (Large leakage).

On each simulation in Wavelet analysis, the first two detail coefficients and the the first approximation coefficient were estimated. In order to estimate internal leakage the RMS values of the detail coefficient d_2 are estimated using Daubechies-8 wavelet as mother wavelet for all cases.

Results are presented from Figure 7.9 to Figure 7.12. Each Figure 7.9 is able to show how detail coefficients d_1 and d_2 are able to capture the system high frequencies with healthy operating conditions.

Different operating pressures where used around in order to make several experiments for each fault case. In every experiment the four simulations were performed.

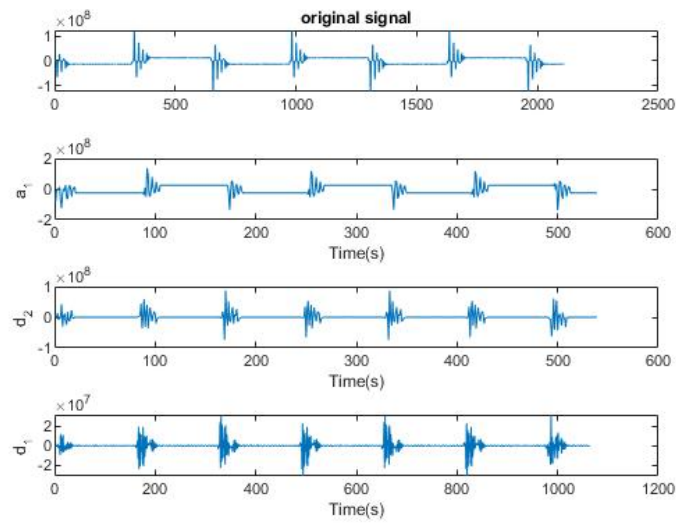


Figure 7.9: Wavelet decomposition, approximation and detail coefficients, no leakage

Figure 7.13 presents the leakage on each fault case, from small leakage to large leakage fault. for each simulation the average leakage was used in the results.

Table 7.2. shows the results for the first experiment, where the normal pressure operating conditions were 12 Mpa or 120 bar. For each simulation the RMS value of detail coefficient d_2 was performed, finally each RMS value was scaled with respect to its normal operating conditions value which in every case was the biggest one since a reduced damping effect takes place.

Four experiments were performed in total, each one simulated the different leakage faults described previously. Results are shown in Figure 7.14 from which the threshold line is clearly identifiable for a good detection of medium leakage faults. At this point the correct separation of healthy and small leakage fault

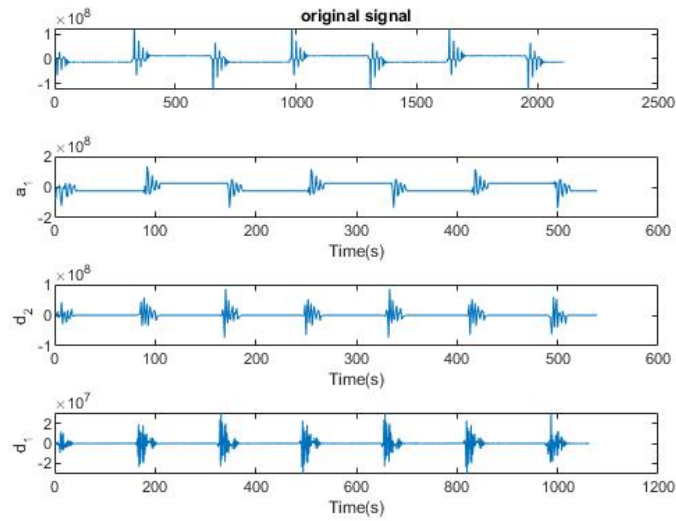


Figure 7.10: Wavelet decomposition, approximation and detail coefficients, small leakage

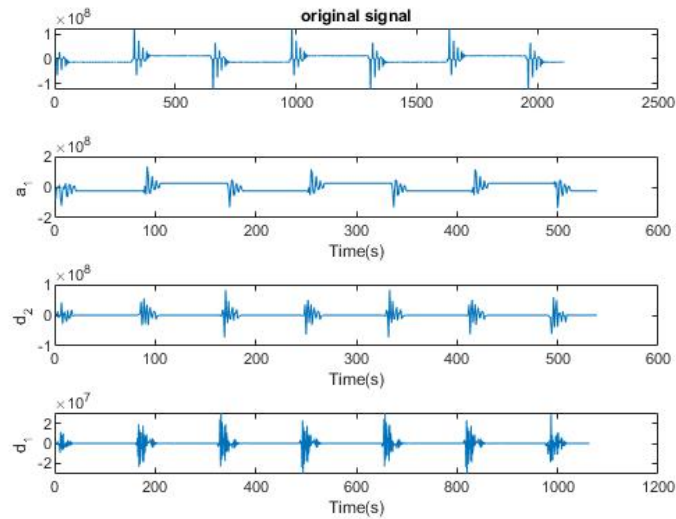


Figure 7.11: Wavelet decomposition, approximation and detail coefficients, medium leakage

conditions is not very clearly distinguished by this methodology. For this reason medium leakage can be identified in a clear manner. It is also noticeable the fact

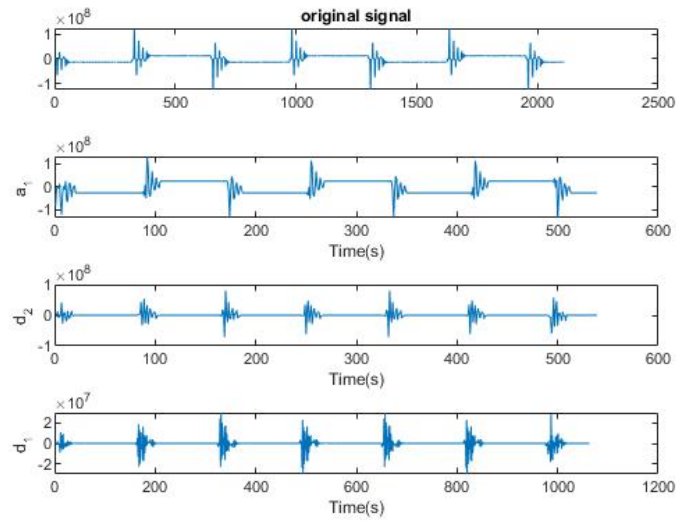


Figure 7.12: Wavelet decomposition, approximation and detail coefficients, large leakage

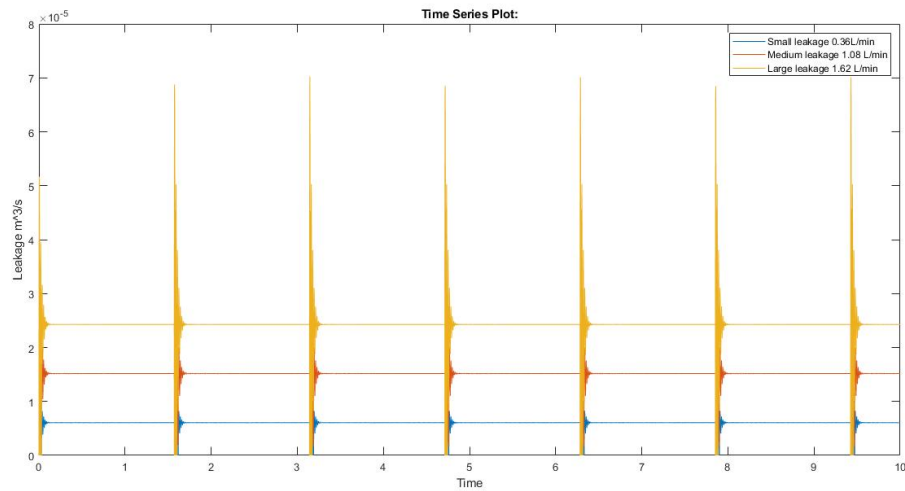


Figure 7.13: Internal leakage computation across the cylinder

that there is a reduction on RMS value at each experiment from no leakage to fault conditions due to the damping effect which increases when more leakage is presented in the internal chambers of the piston, which is captured by the detail coefficient.

Valve opening $\mu\text{ m}$	Leakage level	Mean leakage L/min	RMS scaled d_2	% of change RMS d_2
0	No leak	0	1	0
0.005	small leak	0.36	0.9718	2.823
0.02	medium leak	1.08	0.9316	6.844
0.04	large leak	1.62	0.8958	10.417

Table 7.2: First experiment results with WT methodology for internal leakage detection

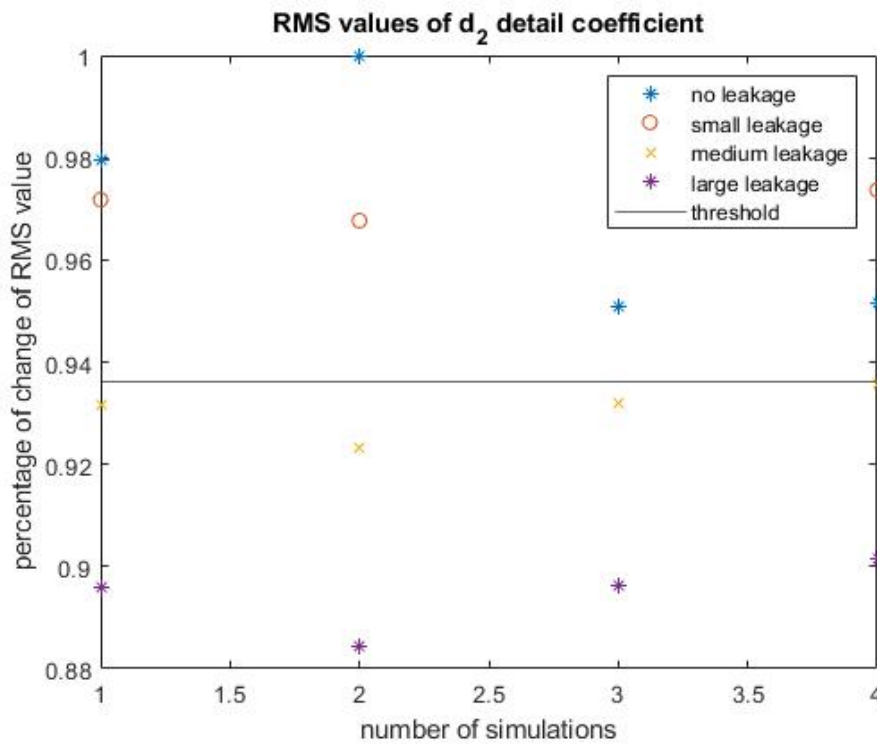


Figure 7.14: WT internal leakage results

7.3.2 Internal leakage Hilbert-Huang decomposition results

The procedure of the experimentation with HHT has the same procedure as WT presented before. This means that four simulations were performed inside four experiments. Each simulation started in normal operating conditions (no leakage fault) to small leakage and finished with large leakage fault conditions.

Empirical Mode Decomposition results are shown in Figure, 7.15 Figure 7.17

to Figure 7.19. It is possible to visualize that in all cases the first IMF captures most of the high frequencies of the pressure signal. Figure 7.16 presents the Instantaneous amplitude computed for normal operating conditions leakage, Here it can be presented in clearer manner how instantaneous amplitude a_1 captures most of the higher frequencies, followed by a_2 and finally a_3 . In a similar manner as the previous case with wavelet decomposition, the damping effect reduces system energy and amplitude if the system has more internal leakage.

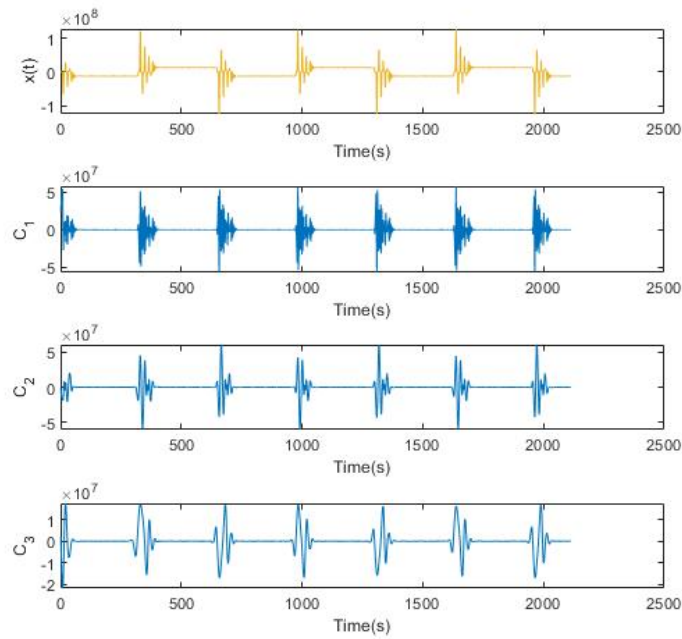


Figure 7.15: Empirical Mode Decomposition of the Pressure signal with no leakage

Table 7.3 shows the results of the first experiment with the four simulations, here it is possible to visualize the reduction in the RMS of the instantaneous amplitude due to internal leakage in the system.

Finally Figure 7.20 shows the result of the four performed experiments. It is possible to see that in comparison with Wavelet methodology, since it can separate adequately small leakage faults from normal operating conditions. Hilbert-Huang transform is able to obtain better results since it appears to be more sensitive to leakage fault detection. However, this methodology is more computationally demanding, this can count as a drawback in certain cases, for instance considering embedded systems for real time analysis.

Valve opening $\mu\text{ m}$	Leakage level	Mean leakage L/min	RMS scaled A_1	% of change RMS A_1
0	No leak	0	1	0
0.005	small leak	0.36	0.952	4.752
0.02	medium leak	1.08	0.917	8.289
0.04	large leak	1.62	0.889	11.078

Table 7.3: First experiment results with HHT methodology for internal leakage detection

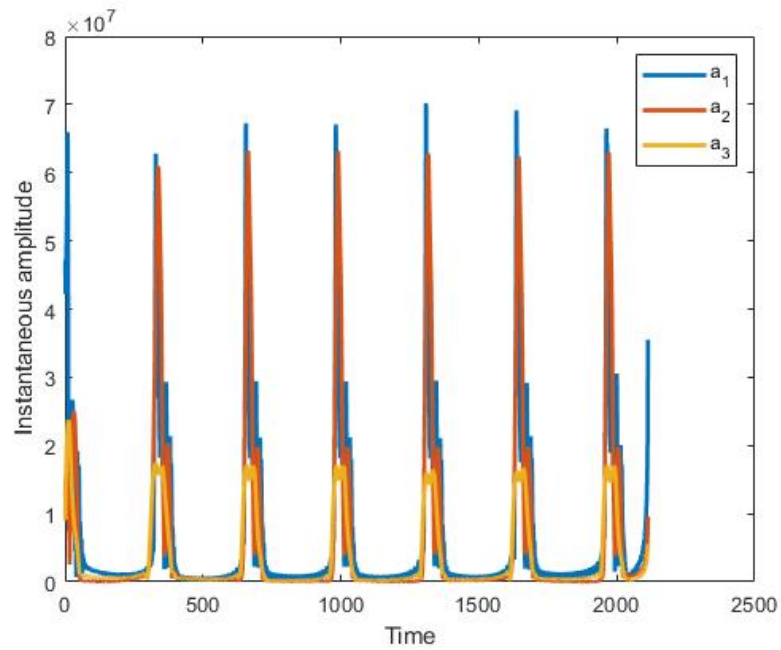


Figure 7.16: Instantaneous Amplitude of the estimated IMF's

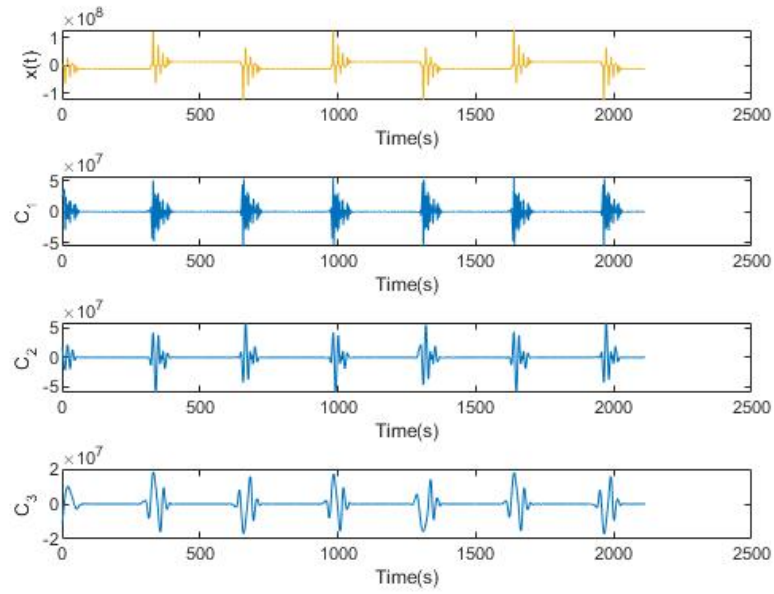


Figure 7.17: IMF's of the Pressure signal with small leakage

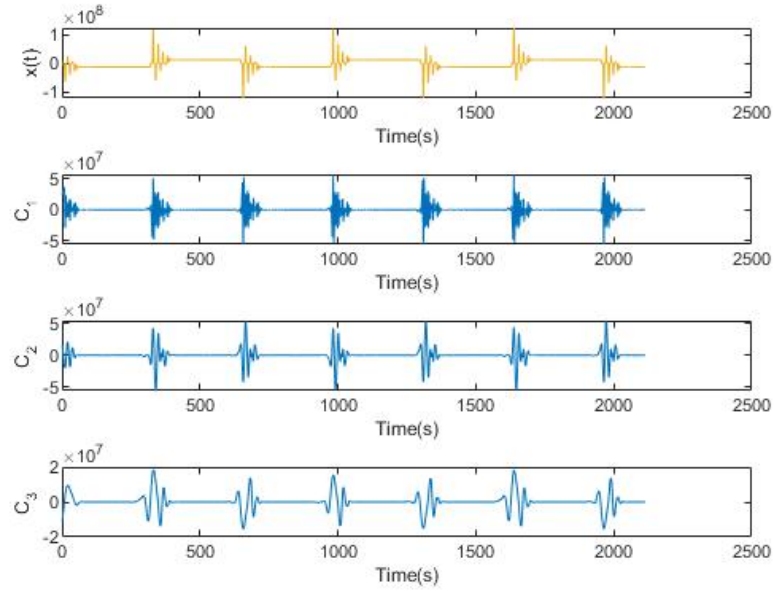


Figure 7.18: IMF's of the Pressure signal with medium leakage

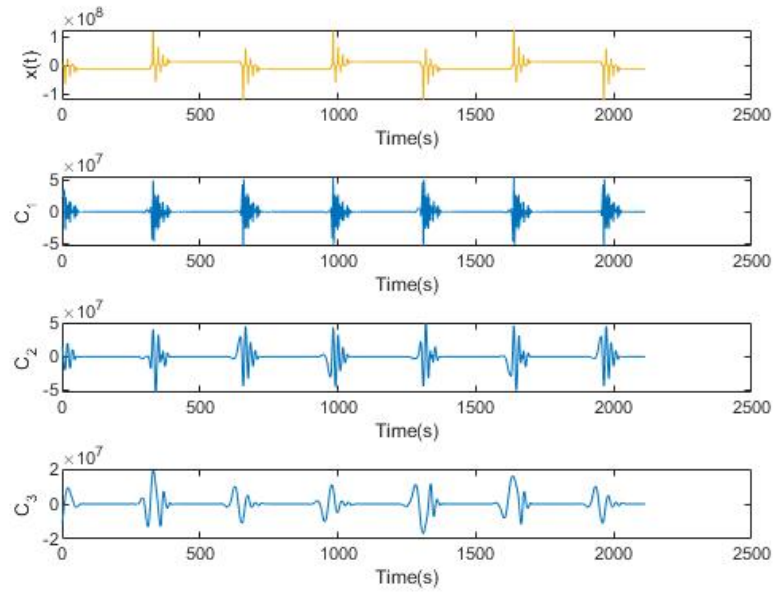


Figure 7.19: IMF's of the Pressure signal with large leakage

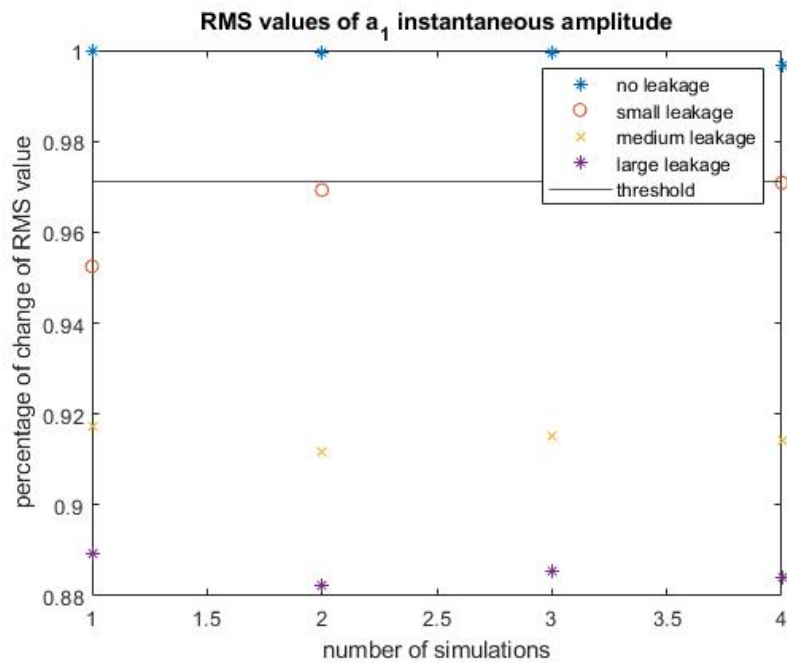


Figure 7.20: HHT internal leakage results

Chapter 8

Conclusions and further works

With regards to the FMEA study performed, and the solutions proposed in this document, the following conclusions can be done The FMEA stated two main problems in the system which were:

- Large compression cylinders leakage fault
- short blade movement cylinders leakage fault
- Wear of rail pads

In order to solve such problems a set of sensors and failure techniques were used. For leakage faults two sets of sensors were used. The first contains sensors with capabilities of reducing the system fault occurrence, such sensors were the LDP100 IFM optical particle detection sensor and the TA310 IFM temperature sensors. Both capable of monitoring the oil health in the system therefore reducing the rate of failure by contaminated oil which leads to leakage. The second set of sensors were used for oil leakage detection, such set of sensors were the mic+25/IU/TC Microsonic Ultrasonic distance measure sensor which was installed in the reservoir to monitor the oil level and the PT5501 IFM pressure sensor used for signal processing techniques.

For the fault due to wear of the rail pads two sensors where used, the Contrinex DW-Ax-509-M18-320 inductive sensor capable of measuring the width of the pads and the ST, STEVAL-STWINKT1B board which has an accelerometer embedded and was used to measure the cylinder misalignment

To collect and send the data, a data acquisition system was built with and Arduino Mega 2560 board which process all sensor data except the accelerometer

data which is processed by a Raspberry PI 4 board. Also a router for WiFi communication and a GPS for positioning were installed.

In order to perform the oil leakage detection, two methodologies were study which involved Wavelet Transform signal decomposition and Hilbert-Huang transform signal decomposition. Since the failure methodologies required failure data which was not available yet by the data acquisition system, dynamic mathematical models were developed for simulating normal and fault conditions (external and internal leakage). From both the pressure signal was used.

The proposed methodology for leakage detection is able to detect leakage failure at a relatively early stage in the case of internal leakage at 0.36 L/min and external leakage of 1.2 L/min rate.

Further studies on this project can be done performing the proposed methodologies with real data, moreover for further analysis, artificial intelligence algorithms such as logistic regression can be performed to the processed data with WT and HHT methodologies for more reliable leakage failure identifications.

Appendix A

Matlab Code external leakage detection

```
%% Generate Faulty data of the hydraulic system

clear all;
close all;
clc;

%% Open Simulink Model
model = 'Ext_leakage_model1';
open_system(model);

d = 0.045e-3 ; % valve opening value

%% Generate Data Ensemble Internal leakage

% Create a Simulink.SimulationInput for each combination of values
siminput = Simulink.SimulationInput(model);

% Modify model parameters
%siminput = setVariable(siminput);

% Collect the simulation input in an array
Internal_Laekage_Sim = siminput;

mkdir Data;
```

```
location = fullfile(pwd,'Data');
[ok,e] = generateSimulationEnsemble(Internal_Laekage_Sim,location,true)

%% Read data from the generated Ensemble

ens = simulationEnsembleDatastore(location)% Save the generated

ensemble into the variable ens
ens.SelectedVariables = ["Pressure1" "Pressure2"];

data1 = read(ens)

%% Plotting measured signal

reset(ens)
ens.SelectedVariables = "Pressure2";

%% Wavelet decomposition

% selecting data for analysis

%while hasdata(ens)

    data = read(ens);
    Pressure2 = data.Pressure2{1};

    % WAVELET TRANSFORM DECOMPOSITION
    [C,L] = wavedec(Pressure2.Data,4,'db8');
    Lev = 4
    a4 = appcoef(C,L,'db8', Lev);
    a3 = appcoef(C,L,'db8',3);
    a2 = appcoef(C,L,'db8',2);
    [d1, d2] = detcoef(C, L, [1 2]);

    % PLOTTING WAVELET DECOMPOSITION OF EACH SIMULATION
```

```
%%
figure,
subplot(4,1,1)
plot(Pressure2.Data);
title('original signal')
xlabel('Time(s)')
ylabel('x(t)')

subplot(4,1,2)
plot(a2);
xlabel('Time(s)')
ylabel('a_2')

subplot(4,1,3)
plot(a3);
xlabel('Time(s)')
ylabel('a_3')

subplot(4,1,4)
plot(a4);
xlabel('Time(s)')
ylabel('a_4')
hold off

RMS_WT_a4 = rms(a4);

%end

RMS_WT = [RMS_WT_a4']
%% Hilbert-Huang transform

reset(ens)
ens.SelectedVariables = "Pressure2";

i = 1;
```

```
%while hasdata(ens)

    data = read(ens);
    Pressure2 = data.Pressure2{1};

    % HILBERT TRANSFORM DECOMPOSITION
    [imf, residual] = emd(Pressure2.Data,'MaxNumIMF', 3); % Empirical Model

    %Decomposition

    [hs,f,t,imfinsf,imfinse] = hht(imf); % Hilbert Huang spectrum
    Inst_Amp = sqrt(imfinse); % Instantaneous Amplitude

    % PLOTTING HILBERT TRANSFORM DECOMPOSITION

    [m n] = size(imf);
    figure,
        for k = 1:n
            subplot(n+1,1,1)
            plot(Pressure2.Data);
            xlabel('Time(s)')
            ylabel('x(t)')

            hold on
            subplot(n+1,1,k+1)
            plot(imf(:,k));
            xlabel('Time(s)')
            ylabel(sprintf('C_%d', k))

        end

        hold off

    % RMS value computation of the instantaneous amplitudes
    RMS_HHT_a1 = rms(Inst_Amp(:,1));
    RMS_HHT_a2 = rms(Inst_Amp(:,2));
    RMS_HHT_a3 = rms(Inst_Amp(:,3));
```

```
%end

RMS_HHT = [RMS_HHT_a1' RMS_HHT_a2' RMS_HHT_a3'];

%% Results
s1 = [1 0.976843164730739 0.929824077337355 0.865495888183081];
s2 = [0.99574 0.976466117187189 0.92978650288463 0.872118154082895]
s3 = [0.97631 0.975759051490528 0.923790486630775 0.879101102532118]
s4 = [0.981 0.976382400306343 0.928289960939136 0.875625777320053]
s5 = [0.98227 0.975243195556626 0.929518871208801 0.882338413060891]

exp = [1 2 3 4 5];
s = [s1;s2;s3;s4;s5];
figure,
plot(exp,s(:,1),'*');
hold on
plot(exp,s(:,2),'o');
hold on
plot(exp,s(:,3),'x');
hold on
plot(exp,s(:,4),'*');

hold off

%% Results
exp = [1 2 3 4 5]';
s1 = [1 0.982271677111502 0.971980074399119 0.961494656484313];
s2 = [0.991614968214892 0.989589420880689 0.967039288195266,...

...,0.955779607958252];
s3 = [0.976312874393088 0.973254520733853 0.962909398855348,...

...,0.953076348002357];
s4 = [0.981001561113864 0.978441055402688 0.968357410930198,...

...,0.957910557501217];
s5 = [0.984594671382198 0.982271677111502 0.971980074399119,...
```

```
...,0.961494656484313];
s = [s1;s2;s3;s4;s5]

figure,
plot(exp,s(:,1),'*');
hold on
plot(exp,s(:,2),'o');
hold on
plot(exp,s(:,3),'x');
hold on
plot(exp,s(:,4),'*');
yline(0.97198)
hold off
xlabel('number of simulations')
ylabel('percentage of change of RMS value')
legend('no leakage','small leakage','medium leakage','large leakage',...
..., 'threshold')
```

Appendix B

Matlab Code Internal leakage detection

```
%%
clear all
close all
clc

s =tf('s');
%% system parameters

m = 200 % mass of the piston rod and other loads kg
d = 6000 % viscous damping coefficient N-sec/m
Beta1 = 689e6; % Bulk modulus Pa
A = 6.33e-4 % Annulus area of the piston m^2
V = 4.68e-4; % Total cylinder volume m^3
rho = 847; % fluid density kg/m^3
c_leak = 0.7; % leakage orifice discharge coefficient
Ps = 17.2e6; % Suply pressure Pa

Cv = 0.6; % Servoalve coefficient discharge
w = 20.75/1000; % servoalve gradient coefficient
Kf1 = 1.02;
Ktp1 = 0;
wh = sqrt((4*Beta1*A^2)/(m*V)); % hydraulic natural frequency
zeta_h = ((wh*V*d)/(8*Beta1*A^2))+((wh*m*Ktp1)/(2*A^2)) % hydraulic
damping coefficient
```

```

%% Non leakage

H1 = (m*s+d)*Kf1*wh^2/A^2;
G1 = s^2+2*zeta_h*wh*s+wh^2;

Y1=H1/G1;

%% leakage system small leakage 0.36 L/min

Plo = 12.5e6 % Load pressure Pa
a_leak2 = 0.05e-6;
h2 = sqrt( a_leak2*4/pi());
xvo = 0.005;

Kf2_o = Cv*w*sqrt((Ps-(xvo*Plo))/rho)
Ktp2_o = ((c_leak*a_leak2)/(sqrt(2*rho)))*((sqrt(Plo)/(Ps-Plo))+1/(sqrt(Plo)))

Kf2 = 1.02;
Ktp2 = 4.54e-11;
Beta2= 689e6;

wh = sqrt((4*Beta2*A^2)/(m*V)); % hydraulic natural frequency
zeta_h = ((wh*V*d)/(8*Beta2*A^2))+((wh*m*Ktp2_o)/(2*A^2)) % hydraulic
damping coefficient

H2 = (m*s+d)*Kf2*wh^2/A^2;
G2 = s^2+2*zeta_h*wh*s+wh^2;

Y2 = H2/G2;

%% leakage system medium leakage 1.08 L/min or 1.8e-5 m^3/s

% Load pressure Pa
a_leak3 = 0.125e-6;
h3 = sqrt( a_leak3*4/pi());

```

```

xvo = 0.005;

Kf3_o = Cv*w*sqrt((Ps-(xvo*Plo))/rho)
Ktp3_o = ((c_leak*a_leak3)/(sqrt(2*rho)))*((sqrt(Plo)/(Ps-Plo))+1/(sqrt(Plo)))

Kf3 = 1.02;
Ktp3 = 4.54e-11;
Beta2= 689e6;

wh = sqrt((4*Beta2*A^2)/(m*V)); % hydraulic natural frequency
zeta_h = ((wh*V*d)/(8*Beta2*A^2))+((wh*m*Ktp3_o)/(2*A^2)) % hydraulic
damping coefficient

H3 = (m*s+d)*Kf3*wh^2/A^2;
G3 = s^2+2*zeta_h*wh*s+wh^2;

Y3 = H3/G3;

% leakage system LARGE leakage 1.62 L/min or 2.6 e-5 m^3/s

a_leak4 = 0.2e-6;
h4 = sqrt( a_leak4*4/pi());
xvo = 0.005;

Kf4_o = Cv*w*sqrt((Ps-(xvo*Plo))/rho)
Ktp4_o = ((c_leak*a_leak4)/(sqrt(2*rho)))*((sqrt(Plo)/(Ps-Plo))+1/(sqrt(Plo)))

Kf4 = 1.02;
Ktp4 = 4.54e-11;
Beta2= 689e6;

wh = sqrt((4*Beta2*A^2)/(m*V)); % hydraulic natural frequency
zeta_h = ((wh*V*d)/(8*Beta2*A^2))+((wh*m*Ktp4_o)/(2*A^2)) % hydraulic
damping coefficient

```

```
H4 = (m*s+d)*Kf4*wh^2/A^2;
G4 = s^2+2*zeta_h*wh*s+wh^2;

Y4 = H4/G4;

% Run simulink simulation
open('int_leakage_sim')
sim('int_leakage_sim')

%% Plotting results

figure,
plot(out.P1, 'LineWidth',2)
hold on
plot(out.P2, 'LineWidth',2)
plot(out.P3, 'LineWidth',2)
plot(out.P4, 'LineWidth',2)
xlabel('Time')
ylabel('Pressure')
legend('No leakage fault','Small leakage fault','Medium leakage fault',...
..., 'Large leakage fault')
hold off

figure,
plot(out.q1)
hold on
plot(out.q2)
plot(out.q3)
xlabel('Time')
ylabel('Leakage m^3/s')
legend('Small leakage 0.36L/min','Medium leakage 1.08 L/min','Large leakage 1.6

hold off

%% Wavelet analysis
[C,L] = wavedec(out.P1.Data,2,'db8');
a2 = appcoef(C,L,'db8',2);
```

```
[d1, d2] = detcoef(C, L, [1 2]);

figure,
subplot(4,1,1)
plot(out.P1.Data);
title('original signal')

subplot(4,1,2)
plot(a2);
xlabel('Time(s)')
ylabel('a_1')

subplot(4,1,3)
plot(d2);
xlabel('Time(s)')
ylabel('d_2')

subplot(4,1,4)
plot(d1);
xlabel('Time(s)')
ylabel('d_1')
hold off

RMS_WT_d1 = rms(d1);
RMS_WT_d2 = rms(d2)
RMS_WT = [RMS_WT_d1 RMS_WT_d2]

%% Hilbert-Huang decomposition
close all

[imf, residual] = emd(out.P4.Data,'MaxNumIMF', 3); % Empirical Mode
Decomposition

[hs,f,t,imfinsf,imfinse] = hht(imf); % Hilbert Huang spectrum
Inst_Amp = sqrt(imfinse); % Instantaneous Amplitude
% PLOTTING HILBERT TRANSFORM DECOMPOSITION
```

```
[m n] = size(imf);
figure,
    for k = 1:n
        subplot(n+1,1,1)
        plot(out.P4.Data);
        xlabel('Time(s)')
        ylabel('x(t)')

        hold on
        subplot(n+1,1,k+1)
        plot(imf(:,k));
        xlabel('Time(s)')
        ylabel(sprintf('C_%d', k))

end

    hold off

    figure,
    plot(Inst_Amp(:,1), 'LineWidth',2)
    hold on
    plot(Inst_Amp(:,2), 'LineWidth',2)
    plot(Inst_Amp(:,3), 'LineWidth',2)
    legend('a_1','a_2','a_3')
    xlabel('Time')
    ylabel('Instantaneous amplitude')
    % RMS value computation of the instantaneous amplitudes
    RMS_HHT_a1 = rms(Inst_Amp(:,1));
    RMS_HHT_a2 = rms(Inst_Amp(:,2));
    RMS_HHT_a3 = rms(Inst_Amp(:,3));

    RMS_HHT = [RMS_HHT_a1 RMS_HHT_a2 RMS_HHT_a3];

%% Plotting results WT

s1= [0.979440988831183 0.97177257471164 0.931564801582436
```

```
...,0.89582865872354];
s2= [1 0.967663031518601 0.923147660363594 0.884290677021685];

s3= [0.950990052946362 0.97199781496325 0.932026419352251

...,0.896280672521688];
s4= [0.951629333513537 0.973667399439366 0.935783703510547

...,0.901684579759185];
s = [s1; s2; s3; s4];
exp =[1 2 3 4];

figure,
plot(exp,s(:,1),'*');
hold on
plot(exp,s(:,2),'o');
plot(exp,s(:,3),'x');
plot(exp,s(:,4),'*');
yline(0.936)
hold off

title ('RMS values of d_2 detail coefficient')
xlabel('number of simulations')
ylabel('percentage of change of RMS value')
legend('no leakage','small leakage','medium leakage','large leakage',...
..., 'threshold')

%% Plotting results HT

s1= [1 0.952482244993642 0.917110519887875 0.889217745283995];
s2= [0.999373581219338 0.969257530850084 0.911614134457348

...,0.882411433427811];
s3= [0.999622842893411 0.972316986102317 0.915220259832781

...,0.885398641089616];
s4= [0.996783363752347 0.970869218746212 0.914085584203687
```

```
...,0.88409837483698];
s = [s1; s2; s3; s4];
exp =[1 2 3 4];

figure,
plot(exp,s(:,1),'*');
hold on
plot(exp,s(:,2),'o');
plot(exp,s(:,3),'x');
plot(exp,s(:,4),'*');
yline(0.971)
hold off

title ('RMS values of a_1 instantaneous amplitude')
xlabel('number of simulations')
ylabel('percentage of change of RMS value')
legend('no leakage','small leakage','medium leakage','large leakage',...
..., 'threshold')
```

Bibliography

- [1] Diomidis H Stamatis. *Failure mode and effect analysis: FMEA from theory to execution*. Quality Press, 2003 (cit. on p. 10).
- [2] Vignesh V Shanbhag, Thomas JJ Meyer, Leo W Caspers, and Rune Schlanbusch. «Failure Monitoring and Predictive Maintenance of Hydraulic Cylinder—State-of-the-Art Review». In: *IEEE/ASME Transactions on Mechatronics* 26.6 (2021), pp. 3087–3103 (cit. on pp. 19, 20, 22, 59).
- [3] Felix Ng, Jennifer A Harding, and Jacqueline Glass. «Improving hydraulic excavator performance through in line hydraulic oil contamination monitoring». In: *Mechanical Systems and Signal Processing* 83 (2017), pp. 176–193 (cit. on p. 19).
- [4] Amin Yazdanpanah Goharrizi and Nariman Sepehri. «A wavelet-based approach to internal seal damage diagnosis in hydraulic actuators». In: *IEEE transactions on industrial electronics* 57.5 (2009), pp. 1755–1763 (cit. on pp. 21, 78, 79).
- [5] Amin Yazdanpanah Goharrizi and Nariman Sepehri. «A wavelet-based approach for external leakage detection and isolation from internal leakage in valve-controlled hydraulic actuators». In: *IEEE Transactions on industrial electronics* 58.9 (2010), pp. 4374–4384 (cit. on pp. 21, 58, 61, 75).
- [6] Amin Yazdanpanah Goharrizi and Nariman Sepehri. «Internal leakage detection in hydraulic actuators using empirical mode decomposition and Hilbert spectrum». In: *IEEE Transactions on Instrumentation and Measurement* 61.2 (2011), pp. 368–378 (cit. on pp. 21, 57).
- [7] Norden E Huang, Zheng Shen, Steven R Long, Manli C Wu, Hsing H Shih, Quanan Zheng, Nai-Chyuan Yen, Chi Chao Tung, and Henry H Liu. «The empirical mode decomposition and the Hilbert spectrum for nonlinear and non-stationary time series analysis». In: *Proceedings of the Royal Society of London. Series A: mathematical, physical and engineering sciences* 454.1971 (1998), pp. 903–995 (cit. on p. 55).

- [8] SJ Loutridis. «Damage detection in gear systems using empirical mode decomposition». In: *Engineering Structures* 26.12 (2004), pp. 1833–1841 (cit. on p. 55).
- [9] Noah D Manring and Roger C Fales. *Hydraulic control systems*. John Wiley & Sons, 2019 (cit. on p. 61).
- [10] Mark Karpenko and Nariman Sepehri. «Fault-tolerant control of a servohydraulic positioning system with crossport leakage». In: *IEEE transactions on control systems technology* 13.1 (2004), pp. 155–161 (cit. on pp. 61, 79).